

Electronic Thesis and Dissertation Repository

---

4-11-2023 9:30 AM

# The Development and Application of a Novel Index for Assessing Vascular Health Status

Nithin J. Menon, *Western University*

Supervisor: Frisbee, Jefferson C, *The University of Western Ontario*

A thesis submitted in partial fulfillment of the requirements for the Master of Science degree in Medical Biophysics

© Nithin J. Menon 2023

Follow this and additional works at: <https://ir.lib.uwo.ca/etd>

---

## Recommended Citation

Menon, Nithin J., "The Development and Application of a Novel Index for Assessing Vascular Health Status" (2023). *Electronic Thesis and Dissertation Repository*. 9227.  
<https://ir.lib.uwo.ca/etd/9227>

This Dissertation/Thesis is brought to you for free and open access by Scholarship@Western. It has been accepted for inclusion in Electronic Thesis and Dissertation Repository by an authorized administrator of Scholarship@Western. For more information, please contact [wlsadmin@uwo.ca](mailto:wlsadmin@uwo.ca).

## Abstract

This thesis addresses the challenge of understanding and evaluating cerebrovascular dysfunction in animal models of depression by introducing a novel approach to establishing and validating a composite metric of vascular function, the vascular health index (VHI). VHI integrates markers of vascular reactivity, vascular wall mechanics, and microvascular network density, providing a reliable and consistent assessment of this important aspect of brain function. This thesis demonstrates the validity and utility of VHI in evaluating integrated vascular function and the effectiveness of interventions to improve microvascular function. This comprehensive approach addresses the need for a standardized metric for cerebrovascular dysfunction, allowing for more accurate evaluation of the extent of vascular impairment throughout the course of chronic conditions like depression, metabolic syndrome and so on. VHI provides researchers with a valuable tool for gaining insight into the efficacy of interventions to improve microvascular function and developing new treatments and therapies for complex disorders.

## Keywords

Data analytics; vascular disease; vascular dysfunction; vascular health outcomes; microcirculation; novel metrics; vascular biology; vascular health and disease.

## Summary for Lay Audience

This thesis is about understanding and evaluating the health of the blood vessels that supply the brain with oxygen and nutrients, and how this is related to depression. We know that changes in blood vessel function can contribute to the development of depressive symptoms but measuring this accurately in animal models of depression has been challenging. To address this issue, we introduce a new approach called the vascular health index (VHI), which integrates different markers of vascular health to provide a more complete picture. By using the VHI, researchers can better evaluate how well the blood vessels are working during depression, and how effective different treatments are in improving blood vessel health. This could help develop new treatments for depression that target blood vessel health. The thesis shows that the VHI can be a useful tool for researchers to better understand and treat chronic conditions underpinned by vascular dysfunction.

## Co-Authorship Statement

This thesis integrated the following two published papers into its two body chapters.

- Menon NJ, Halvorson BD, Alimorad GH, Frisbee JC, Lizotte DJ, Ward AD, Goldman D, Chantler PD, Frisbee SJ. A novel vascular health index: Using data analytics and population health to facilitate mechanistic modeling of microvascular status. *Front Physiol.* 2022 Dec 6;13:1071813. doi: 10.3389/fphys.2022.1071813. PMID: 36561210; PMCID: PMC9763931.
- Menon NJ, Halvorson BD, Alimorad GH, Frisbee JC, Lizotte DJ, Ward AD, Goldman D, Chantler PD, Frisbee SJ. Application of a novel index for understanding vascular health following pharmacological intervention in a pre-clinical model of metabolic disease. *Front Pharmacol.* 2023 Jan 25;14:1104568. doi: 10.3389/fphar.2023.1104568. PMID: 36762103; PMCID: PMC9905672.

## Acknowledgments

I would first like to thank my family. Their unwavering support, love, and encouragement have been the backbone of my academic journey. I am grateful to my parents and brother for always believing in me and pushing me to pursue my academic goals.

I want to thank Jeff for his exceptional mentorship, for anticipating my needs, and for providing me with guidance that has not only helped me succeed in research but has also contributed to my personal growth. His exceptional insights, patience, and encouragement have been invaluable to me.

I would also like to thank Stephanie for her constant support and generosity with her time and insights. Stephanie's unwavering technical, statistical, and moral support have been integral to my progress and have helped me navigate the challenges of this thesis. I admire her productivity and aspire to emulate her and Jeff's efforts as mentors and P.I.s.

I am also grateful to Brayden for welcoming me into the lab and supporting me throughout my master's degree. His guidance, encouragement, and mentorship have been invaluable to me.

Finally, I would like to thank my advisory committee for their timely insights, feedback, and support. Their expertise and guidance have been instrumental in shaping my research and helping me achieve my academic goals.

To all those who have supported me, encouraged me, and helped me in countless ways throughout my academic journey, I extend my heartfelt gratitude.

# Table of Contents

Abstract	ii
Summary for Lay Audience	iii
Co-Authorship Statement	iv
Acknowledgments	v
Table of Contents	vi
List of Tables	viii
List of Figures	ix
Chapter 1	1
1 General Introduction	1
<b>1.1 Overview</b>	<b>2</b>
1.1.1 Animal Models of Depression	2
1.1.2 General effects of depression on cerebral vasculature	3
<b>1.2 Direct measures of Cerebrovascular health</b>	<b>4</b>
1.2.1 Vascular reactivity	4
1.2.2 Micro vessel density (rarefaction)	5
1.2.3 Vascular wall mechanics	6
<b>1.3 Indirect Indicators of Cerebrovascular function</b>	<b>8</b>
1.3.1 Oxidative stress and Inflammation	8
1.3.2 Blood Brain barrier permeability	9
1.3.3 Biomarkers of endothelial dysfunction	10
1.3.4 Cerebral Blood flow	12
<b>1.4 Conclusion</b>	<b>12</b>
<b>1.5 Literature Cited</b>	<b>14</b>
Chapter 2	22
2 Integrated Article 1: A novel vascular health index: Using data analytics and population health to facilitate mechanistic modeling of microvascular status	22

<b>2.1</b>	<b>Introduction</b>	<b>22</b>
<b>2.2</b>	<b>Materials and Methods</b>	<b>25</b>
2.2.1	Animal Model	25
2.2.2	Development of vascular health index (VHI)	31
<b>2.3</b>	<b>Results</b>	<b>38</b>
<b>2.4</b>	<b>Discussion</b>	<b>55</b>
<b>2.5</b>	<b>Literature Cited</b>	<b>63</b>
Chapter 3		67
	Bridge Section	67
3	Integrated article 2: Application of a novel index for understanding vascular health following pharmacological intervention in a pre-clinical model of metabolic disease	68
<b>3.1</b>	<b>Introduction</b>	<b>68</b>
<b>3.2</b>	<b>Materials and Methods</b>	<b>70</b>
3.2.1	Animal Model	71
3.2.2	Determining VHI characteristics	75
<b>3.3</b>	<b>Results</b>	<b>82</b>
<b>3.4</b>	<b>Discussion</b>	<b>94</b>
<b>3.5</b>	<b>Literature Cited</b>	<b>100</b>
4	Conclusion	104
	Curriculum Vitae	108

## List of Tables

Table 2-1: Calculations of VHI Components .....	37
Table 2-2: Sample sizes of present study.....	38
Table 2-3: Animal baseline characteristics .....	40
Table 2-4: Peripheral (skeletal muscle) vascular component data.....	42
Table 2-5: Cerebral vascular component data .....	43
Table 2-6: Calculated vascular health index (VHI) .....	45
Table 3-1: VHI Component calculation.....	81
Table 3-2: Animal sample sizes for all treatment groups .....	82
Table 3-3: Animal baseline characteristics .....	83
Table 3-4: Skeletal muscle vascular component data.....	85
Table 3-5: Cerebral vascular component data .....	87



## List of Figures

Figure 2-1: Schematic representation of the VHI components.....	34
Figure 2-2: 5 parameter peripheral (skeletal) VHI data.....	47
Figure 2-3: 3 parameter VHI of peripheral (skeletal muscle) microcirculation .....	49
Figure 2-4: 5 parameter VHI of cerebral circulation .....	50
Figure 2-5: 3 parameter VHI for cerebral microcirculation.....	51
Figure 2-6: TNF- $\alpha$ and Plasma Insulin correlations with peripheral VHI .....	53
Figure 2-7: TNF- $\alpha$ and Plasma Insulin Correlations with Cerebral VHI.....	54
Figure 3-1: VHI Component schematic .....	76
Figure 3-2: 3 parameter VHI data in skeletal muscle microcirculation.....	89
Figure 3-3: TNF- and plasma insulin correlations with peripheral VHI .....	91
Figure 3-4: Cerebral microcirculation VHI data.....	92
Figure 3-5: TNF- and plasma insulin correlations with cerebral VHI.....	94

# Chapter 1

## 1 General Introduction

Depression is a rampant and debilitating mental health disorder affecting millions of people worldwide. The use of animal models in the study of depression has enabled the discovery of valuable insights into the underlying mechanisms and potential treatments for this disorder. Recent studies have suggested a link between depression and cerebrovascular dysfunction [1]. This relationship has significant implications for our understanding of depression and its underlying causes, as well as for the development of new treatments.

Several animal models have been developed to study the relationship between depression and cerebrovascular dysfunction. For example, the chronic mild stress (CMS) model in rats [2] and the social defeat model [3] in mice have been widely used to induce depression-like behavior and to assess cerebrovascular dysfunction.

However, one of the challenges in synthesizing the existing literature on this topic is the heterogeneity in how cerebrovascular dysfunction is measured, quantified, and evaluated [4]. Different studies have used a variety of techniques and indicators, such as cerebral blood flow measures, blood brain barrier permeability, and oxidative stress markers to evaluate cerebrovascular function in animal models of depression. This heterogeneity makes it challenging to compare results across studies and to accurately assess the extent of cerebrovascular dysfunction in depression.

This introductory chapter aims to outline the existing research on the relationship between depression and cerebrovascular dysfunction in animal models, with a focus on the heterogeneity in how cerebrovascular dysfunction is measured and evaluated. This chapter will aim to identify gaps in the literature and to provide a foundation for future research in this area, including the development of standardized methods for assessing cerebrovascular dysfunction in animal models of depression.

## 1.1 Overview

### 1.1.1 Animal Models of Depression

The development of translationally relevant animal models has greatly facilitated the investigation of the connection between chronic stress/depression and the development of vascular dysfunction. These preclinical models of depression were developed to maximize their similarity to the etiology and progression of clinical depression, and capability of the model to replicate morphological, biochemical, and behavioral features of human pathology [5]. The learned helplessness model, the early life stress model [6], the social defeat model [7], and the unexpected chronic mild stress (UCMS) model are some of the preclinical models of depression that are most frequently employed in behavioral research [2]. Based on its capacity to mimic the emergence of numerous human clinical depressed symptoms, such as anhedonia and learned helplessness, the UCMS protocol is often regarded as the most suitable rat model for human clinical depression [2]. According to the UCMS model, daily minor stressors are repeatedly and randomly exposed, leading to a cumulative stress response over time. By these methods, animals are subjected to daily modest environmental and social stressors for a period of eight weeks [8]. The high degree of unpredictability and uncontrollability of the stressors experienced over an extended period, without posing life-threatening or difficult challenges to the animals, is a critical differentiating factor that improves the translational relevance of this model to chronic stress in humans [9]. The foundation of the UCMS model is the idea that long-term exposure to unpredictable, exogenous stressors eventually results in the emergence of depressive symptoms resembling those of clinical depression, such as decreased reward responsiveness (anhedonia), changes in physical activity and investigative behavior (helplessness and despair) [9], worsening of the coat state, and disrupted sexual activity [8]. Interestingly, prolonged treatment with some antidepressants can progressively correct these changed depressive behaviors but not acute treatment, suggesting similar neurological effects of antidepressants in depressed patients [9].

### 1.1.2 General effects of depression on cerebral vasculature

Depression has been associated with cerebrovascular abnormalities that may contribute to the cognitive and emotional symptoms associated with the disorder. Chronic stress and inflammation are believed to play a significant role in the pathophysiology of depression and the associated cerebrovascular abnormalities [5]. Stress-induced changes in the hypothalamic-pituitary-adrenal (HPA) axis, sympathetic nervous system (SNS), and inflammatory response can lead to the dysregulation of cerebral blood flow and the increased permeability of the blood-brain barrier [5]. The HPA axis is activated by stress and releases corticotrophin-releasing hormone (CRH), which in turn stimulates the release of adrenocorticotrophic hormone (ACTH) from the pituitary gland, leading to the release of glucocorticoids from the adrenal cortex [10]. The resulting increase in glucocorticoid levels can lead to alterations in cerebral blood flow [10], decreased hippocampal neurogenesis, and increased neuronal damage and oxidative stress [11]

The SNS is also activated by stress, leading to increased catecholamine release and vasoconstriction, which can contribute to the dysregulation of cerebral blood flow and increased blood pressure [12]. Chronic sympathetic activation can also lead to endothelial dysfunction and increased oxidative stress in the cerebral vasculature [5]. Inflammation is another key factor in the pathophysiology of depression and associated cerebrovascular abnormalities. Chronic inflammation can lead to the activation of microglia, the release of cytokines [13], and the dysregulation of cerebral blood flow and the blood brain barrier (BBB) [14]. Additionally, inflammation can lead to increased oxidative stress and endothelial dysfunction in the cerebral vasculature, contributing to cerebrovascular dysfunction and cognitive impairment [15].

Overall, hormonal changes associated with the stress response, including those in the HPA axis and SNS, as well as chronic inflammation, can contribute to the cerebrovascular abnormalities observed in depression. Understanding these changes is important for identifying potential therapeutic targets and improving the management of depression and associated cerebrovascular dysfunction.

## 1.2 Direct measures of Cerebrovascular health

### 1.2.1 Vascular reactivity

Vessel reactivity, or the ability of blood vessels to constrict or dilate in response to various stimuli, is an important physiological process that regulates blood flow and blood pressure throughout the body. Measuring vessel reactivity in animal models can provide valuable insights into the mechanisms of vascular dysfunction in states of elevated cerebrovascular disease risk and the effects of potential interventions.

One commonly used method for measuring vessel reactivity in animal models is *in vitro* wire myography. This technique involves dissecting small segments of blood vessels and mounting them on a wire in a tissue bath filled with physiological solution. The vessel is then stimulated with various vasoactive agents, such as acetylcholine, norepinephrine, or potassium chloride, and the resulting changes in vessel diameter are computed using specialized equipment that accounts for tension under isometric conditions [16]. Another method is Doppler ultrasound, which can be used to measure blood flow velocity and vessel diameter *in vivo*. This technique has been used to assess vessel reactivity in various animal models, including rats and mice [17].

There are generally two types of vessel reactivity that can be measured: endothelium-dependent and endothelium-independent reactivity. Endothelium-dependent reactivity refers to the ability of blood vessels to dilate in response to substances released by the endothelium, the inner lining of blood vessels. One common substance released by the endothelium is nitric oxide (NO), which is a potent vasodilator. Other substances, such as prostacyclin and endothelium-derived hyperpolarizing factor (EDHF), also contribute to endothelium-dependent dilation [18].

Endothelium-independent reactivity, on the other hand, refers to the ability of blood vessels to dilate in response to substances that act directly on the smooth muscle cells of the vessel wall, rather than via the endothelium. One commonly used substance for assessing endothelium-independent reactivity is sodium nitroprusside (SNP), which acts directly on smooth muscle cells to induce vasodilation. Endothelium-independent

reactivity can be assessed using techniques such as SNP-induced dilation or potassium chloride-induced constriction [19].

Measuring both types of reactivity can provide important information about the overall function of the vascular system and can help to identify specific mechanisms that may be impaired in various states of elevated cerebrovascular dysfunction. For example, in models of chronic stress with elevated levels of glucocorticoids like cortisol, vascular reactivity is impacted through both endothelial and vascular smooth muscle cells. The bioavailability of nitric oxide (NO, a potent vasodilator) is decreased significantly as a result of increased cortisol levels in two ways: directly by blocking endothelial NO synthase (eNOS), and indirectly by causing more oxidative stress [5].

The ultimate effect is that in the UCMS model of depression, large proximal arteries of the cerebrovascular network undergo significant pathological adaptations that lead to severely impaired vessel reactivity [5]. One study showed that with 8 weeks of chronic stress in lean male Zucker rats, they observed significantly reduced endothelial dependent vasodilation of the middle cerebral artery (MCA) to acetylcholine, as well as a heightened MCA constriction response to serotonin (a potent cerebrovascular constrictor) [5].

### 1.2.2 Micro vessel density (rarefaction)

Microvessel rarefaction refers to a reduction in the density of small blood vessels, or capillaries, in a particular tissue. This can lead to decreased blood flow and oxygen delivery to the tissue, which can have important implications for tissue function and health. Microvessel rarefaction has been implicated in various diseases, including cardiovascular disease, diabetes, and depression [20].

One method for measuring microvessel rarefaction in animal models is to use stereological analysis, which involves quantifying the number and density of capillaries in a particular tissue using unbiased sampling techniques. This method involves staining the tissue with a specific marker, such as an antibody against a vascular marker like CD31 and using specialized imaging software to analyze the images.

Another method for measuring micro vessel rarefaction in animal models is to use in vivo imaging techniques, such as laser speckle contrast imaging (LSCI) or optical coherence tomography (OCT) [21]. These techniques allow for non-invasive imaging of blood flow and vessel density in real-time [21].

Measuring micro-vessel rarefaction in animal models of depression can provide important insights into the pathophysiology of the disease and the potential mechanisms underlying its various symptoms, such as cognitive impairment and emotional dysregulation. It can also help to identify potential therapeutic targets for treating depression and associated vascular dysfunction.

Neovascularization is a process through which tissues adapt to numerous stimuli through angiogenesis (new vessel production from existing vessels) and arteriogenesis (collateral remodeling) [5]. This process is negatively impacted under conditions of chronic stress as seen in a study that showed that 8 weeks of UCMS significantly reduced the brain micro vessel density in male lean rats [5]. The specific mechanism of this decrease in angiogenesis in the brain is not completely uncovered yet.

Arteriogenesis and angiogenesis are both strongly influenced by environmental stimuli, and they most likely differ in healthy and diseased states. One previous investigation into the physiological mechanisms causing microvascular rarefaction in the brain has pointed to the delicate balance between oxidative stress and endothelial function (such as altered arachidonic acid metabolism and NO bioavailability) as a major factor in the development and severity of microvascular rarefaction in conditions of chronic stress [20]. Furthermore, the expression of vascular endothelial growth factors (VEGF) is crucial for these activities. The evidence implies that thrombospondin-1 (TSP-1) is a key factor in capillary regression and pathologically caused rarefaction, whereas VEGF is a crucial trigger to start angiogenesis [22].

### 1.2.3 Vascular wall mechanics

Cerebral vascular wall mechanics refer to the physical properties of the blood vessels in the brain, such as their stiffness, compliance, and elasticity. Changes in cerebral vascular

wall mechanics have been observed in various neurological and psychiatric disorders, including depression [23]. In animal models of depression, cerebral vascular wall mechanics can be measured using various techniques.

One commonly used technique to measure cerebral vascular wall mechanics in animal models is pressure myography. Pressure myography involves the perfusion of isolated cerebral vessels with a physiological salt solution, while simultaneously measuring the internal diameter of the vessel in response to changes in intraluminal pressure. This allows for the calculation of various mechanical parameters, such as vessel wall thickness, distensibility, and compliance [24].

Another technique used to measure cerebral vascular wall mechanics in animal models is atomic force microscopy (AFM). AFM involves the use of a small cantilever with a sharp tip to measure the mechanical properties of the vascular wall, including its stiffness and elasticity. AFM can provide high-resolution images of the vascular wall and allows for the measurement of topographical and mechanical properties at the nanoscale level [25].

In addition, ultrasound imaging can be used to measure cerebral vascular wall mechanics in animal models of depression. Ultrasound imaging can provide real-time images of the cerebral vasculature and allow for the measurement of various mechanical parameters, such as wall thickness [26], blood flow velocity and volume [27].

Measuring cerebral vascular wall mechanics in animal models of depression can provide important insights into the underlying mechanisms of cerebrovascular dysfunction in the disorder. Changes in vascular wall mechanics can contribute to alterations in cerebral blood flow and BBB permeability, leading to neuronal damage and cognitive impairment [28, 29]. Understanding these changes can help identify potential therapeutic targets for treating depression and associated cerebrovascular dysfunction.



## 1.3 Indirect Indicators of Cerebrovascular function

### 1.3.1 Oxidative stress and Inflammation

Oxidative stress and inflammation are two related processes that can lead to dysfunction in the cerebral vasculature, thereby contributing to the pathophysiology of depression [30–33]. Oxidative stress refers to an imbalance between the production of reactive oxygen species (ROS) and the ability of the body's antioxidant systems to neutralize them [34]. Inflammation, on the other hand, is a response of the immune system to harmful stimuli, such as infection or injury. Both oxidative stress and inflammation can lead to damage to the cerebral vasculature, impairing blood flow and contributing to depressive symptoms [35].

In animal models of depression, oxidative stress and inflammation can be measured using various techniques. For example, the level of ROS can be measured directly using modified proteins and DNA to facilitate immunostaining in intact tissues [36]. These assays measure the levels of ROS in tissue in specific cell populations, such as microglia or astrocytes [37].

Inflammation can be measured using various biomarkers, such as cytokines or chemokines, which are released by immune cells in response to inflammation. These biomarkers can be measured using ELISA or other immunoassays in blood, brain tissue, or cerebrospinal fluid samples [38].

In addition, various imaging techniques, such as magnetic resonance imaging (MRI) or positron emission tomography (PET), can be used to visualize and quantify the extent of oxidative stress and inflammation in the brain. For example, MRI can be used to measure changes in brain tissue structure and function associated with oxidative stress and inflammation [39].

The cerebrovascular maladaptations to chronic stress, such as reduced NO bioavailability in the cerebral vessels, is linked to the oxidative stress and neuroinflammation seen in UCMS [5]. In the pro-oxidative conditions of UCMS, the ratio of dilating and constricting metabolites is significantly altered [5], by shifting arachidonic acid

metabolism to the production of vasoconstricting metabolites, like thromboxane, which will compete with the vasodilatory stimuli from NO, prostacyclin, and other vasodilators [40].

The reduction in NO bioavailability and signalling is a key mechanism for how oxidative stress affects vascular function. Chronically stressful circumstances can cause oxidative stress, which can shift the balance of NO from the predominantly physiologic eNOS mediated creation of NO to the detrimental superoxide generation from NO [41]. This effect can be further exacerbated when, reactive oxygen species activate a pathway leading to redox gene expression, which suppresses mRNA expression of eNOS and eNOS activity [5]. The brain is particularly vulnerable to this imbalance because of its large amounts of peroxidizable fatty acids, lack of antioxidant measures [42], and high oxygen demand [5].

### 1.3.2 Blood Brain barrier permeability

The blood-brain barrier (BBB) is a selectively permeable membrane that separates the blood vessels in the brain from the surrounding brain tissue. The BBB plays a critical role in regulating the exchange of molecules between the blood and the brain, including nutrients, waste products, and therapeutic drugs. Disruption of the BBB permeability can have important implications for brain function and is implicated in various neurological and psychiatric disorders, including depression [43, 44].

In animal models of depression, BBB permeability can be measured using various techniques, such as the Evans blue dye (EBD) extravasation assay or the measurement of tight junction protein expression. The EBD assay involves the injection of EBD into the bloodstream of the animal, which binds to serum albumin and is normally excluded from crossing the BBB [45]. In animals with BBB disruption, such as those exposed to chronic stress or inflammatory stimuli, the EBD leaks out of the blood vessels and accumulates in the surrounding brain tissue [45]. The amount of EBD extravasation can then be quantified using specialized imaging techniques or biochemical assays [45]

Another method for measuring BBB permeability in animal models is to measure the expression of tight junction proteins, which are critical components of the BBB. These proteins, such as occludin and claudin, form tight seals between adjacent endothelial cells and help to maintain the integrity of the BBB [46]. Disruption of tight junction proteins is associated with increased BBB permeability. The expression of tight junction proteins can be measured using techniques such as Western blot or immunohistochemistry.

Blood-brain barrier hyperpermeability has been used as evidence of neurovascular dysfunction in postmortem human, and animal model studies involving oxidative stress and neuroinflammation [5]. Normally, the creation of NO by eNOS raises cellular levels of cyclic guanosine monophosphate, causing endothelium dependent dilation and ultimately improving cerebral blood flow [47]. But when production of NO from iNOS is paired with the presence of superoxides, the blood-brain barrier integrity is severely compromised [5]. From this it is apparent that neurovascular endothelial dysfunction is an upstream contributing factor of BBB hyperpermeability and the use of BBB as an indicator of vascular dysfunction approximates endothelial dysfunction.

### 1.3.3 Biomarkers of endothelial dysfunction

Cerebral endothelial dysfunction refers to impaired function of the cells that line the inner surface of blood vessels in the brain, known as cerebral endothelial cells. The influx of vital nutrients, the efflux of harmful compounds, the ionic homeostasis of the brain interstitial fluid, and the prevention of the brain's influx of peripheral substances, neurotransmitters, etc. are all controlled by the neurovascular endothelium. Endothelial dysfunction can lead to a range of cerebrovascular abnormalities mentioned in the above sections, including decreased blood flow, impaired regulation of blood pressure, and increased blood-brain barrier permeability [48]. In animal models of depression, biomarkers of cerebral endothelial dysfunction can be measured using various techniques. It is important to distinguish these biomarkers from assessing endothelial dysfunction by directly measuring vascular reactivity. One such marker of cerebral endothelial dysfunction is the expression of endothelial nitric oxide synthase (eNOS), an enzyme that plays a key role in regulating cerebral blood flow. Reduced expression of eNOS has been associated with endothelial dysfunction and impaired vascular function in animal models

of depression [49]. The expression of eNOS can be measured using techniques such as Western blot or immunohistochemistry.

Another such marker is the expression of endothelin-1 (ET-1), a potent vasoconstrictor peptide that is produced by endothelial cells. ET-1 has been shown to be elevated in various brain regions in animal models of depression and may contribute to cerebrovascular dysfunction [50]. The expression of ET-1 can be measured using techniques such as ELISA or immunohistochemistry.

In states of chronic stress, the overstimulation of the autonomic nervous system and hypothalamic-pituitary-adrenal axis is associated with an overactivation of the renin-angiotensin system, which leads to increased levels of lipid peroxidation [5]. Lipid peroxidation is a process in which free radicals react with polyunsaturated fatty acids in cell membranes, leading to the production of lipid peroxides and other reactive byproducts. Lipid peroxidation has also been implicated in the pathophysiology of depression. In animal models of depression, products of lipid peroxidation have been used to approximate endothelial dysfunction in the brain [5].

One such product of lipid peroxidation is malondialdehyde (MDA), which is generated by the breakdown of polyunsaturated fatty acids. MDA is a well-established marker of oxidative stress and has been shown to be elevated in various brain regions in animal models of depression [51]. MDA can be measured using techniques such as high-performance liquid chromatography (HPLC) or enzyme-linked immunosorbent assay (ELISA). In addition, isoprostanes, a family of compounds generated by the peroxidation of arachidonic acid, have been used as markers of oxidative stress and endothelial dysfunction in animal models of depression [52]. Isoprostanes can be measured using techniques such as gas chromatography-mass spectrometry or ELISA.

Another marker of cerebral endothelial dysfunction is the expression of adhesion molecules, such as intercellular adhesion molecule-1 (ICAM-1) and vascular cell adhesion molecule-1 (VCAM-1) [53]. Adhesion molecules are critical for leukocyte adhesion and recruitment to sites of inflammation, and their increased expression is indicative of endothelial activation and dysfunction [53]. The expression of adhesion

molecules can be measured using techniques such as Western blot, immunohistochemistry, or flow cytometry.

### 1.3.4 Cerebral Blood flow

Cerebral blood flow (CBF) refers to the amount of blood that flows through the brain's blood vessels in a given period of time. CBF is an important indicator of cerebrovascular function, as it reflects the brain's demand for oxygen and nutrients and is critical for maintaining normal brain function. Impaired CBF regulation and reduced CBF are the outcomes of the cerebrovascular dysfunction that is implicated in various neurological and psychiatric disorders, including depression [54–58].

In animal models of depression, CBF can be measured using various techniques, such as laser Doppler flowmetry. Laser Doppler flowmetry measures changes in blood flow in the brain in response to various stimuli, such as pharmacological agents or changes in oxygen or carbon dioxide levels [59]. This technique involves placing a probe on the skull and measuring changes in the reflection of a laser beam as it passes through the brain tissue [59].

## 1.4 Conclusion

Prolonged exposure to stress, as seen in animal models of depression, has been shown to cause pathological changes in cerebrovascular function, which can contribute to the development of depressive symptoms. However, the methods used to measure and quantify cerebrovascular dysfunction in these studies can vary widely, making it difficult to compare results across studies.

The lack of a standardized metric for cerebrovascular dysfunction also makes it challenging to understand the precise role that cerebrovascular dysfunction plays in the development and treatment of depression. To address this issue, there is a need for a more integrated approach to measuring cerebrovascular health that can provide a reliable and consistent assessment of this important aspect of brain function.

By developing a standardized and integrated metric for cerebrovascular dysfunction, researchers could more accurately evaluate the extent of vascular impairment throughout the course of depression, which could help to inform new treatments and therapies for this complex disorder.

## 1.5 Literature Cited

1. Alexopoulos, G. S. (1997). "Vascular Depression" Hypothesis. *Archives of General Psychiatry*, 54(10), 915.  
<https://doi.org/10.1001/archpsyc.1997.01830220033006>
2. Willner, P. (2005). Chronic Mild Stress (CMS) Revisited: Consistency and Behavioural-Neurobiological Concordance in the Effects of CMS. *Neuropsychobiology*, 52(2), 90–110. <https://doi.org/10.1159/000087097>
3. Krishnan, V., Han, M.-H., Graham, D. L., Berton, O., Renthal, W., Russo, S. J., ... Nestler, E. J. (2007). Molecular Adaptations Underlying Susceptibility and Resistance to Social Defeat in Brain Reward Regions. *Cell*, 131(2), 391–404.  
<https://doi.org/10.1016/j.cell.2007.09.018>
4. Brunner, H., Cockcroft, J. R., Deanfield, J., Donald, A., Ferrannini, E., Halcox, J., ... Webb, D. J. (2005). Endothelial function and dysfunction. Part II: Association with cardiovascular risk factors and diseases. A statement by the Working Group on Endothelins and Endothelial Factors of the European Society of Hypertension\*. *Journal of Hypertension*, 23(2), 233–246. <https://doi.org/10.1097/00004872-200502000-00001>
5. Burrage, E., Marshall, K., Santanam, N., & Chantler, P. (2018). Cerebrovascular dysfunction with stress and depression. *Brain Circulation*, 4(2), 43.  
[https://doi.org/10.4103/bc.bc\\_6\\_18](https://doi.org/10.4103/bc.bc_6_18)
6. Willner, P. (1997). Validity, reliability and utility of the chronic mild stress model of depression: a 10-year review and evaluation. *Psychopharmacology*, 134(4), 319–329. <https://doi.org/10.1007/s002130050456>
7. Morais-Silva, G., Costa-Ferreira, W., Gomes-de-Souza, L., Pavan, J. C., Crestani, C. C., & Marin, M. T. (2019). Cardiovascular outcomes related to social defeat stress: New insights from resilient and susceptible rats. *Neurobiology of Stress*, 11, 100181. <https://doi.org/10.1016/j.ynstr.2019.100181>

8. Nollet, M., Guisquet, A. Le, & Belzung, C. (2013). Models of Depression: Unpredictable Chronic Mild Stress in Mice. *Current Protocols in Pharmacology*, 61(1). <https://doi.org/10.1002/0471141755.ph0565s61>
9. Stanley, S. C. (2015, January 1). *Chronic Stress, Depressive Symptoms and Peripheral Vascular Dysfunction: Fundamentals, Mechanisms, Sex Disparities, and Determinants of Integrated Outcomes*. West Virginia University Libraries.
10. Sapolsky, R. M., Romero, L. M., & Munck, A. U. (2000). How Do Glucocorticoids Influence Stress Responses? Integrating Permissive, Suppressive, Stimulatory, and Preparative Actions\*. *Endocrine Reviews*, 21(1), 55–89. <https://doi.org/10.1210/edrv.21.1.0389>
11. Salim, S. (2014). Oxidative Stress and Psychological Disorders. *Current Neuropharmacology*, 12(2), 140–147. <https://doi.org/10.2174/1570159X11666131120230309>
12. Wortsman, J. (2002). Role of epinephrine in acute stress. *Endocrinology and Metabolism Clinics of North America*, 31(1), 79–106. [https://doi.org/10.1016/S0889-8529\(01\)00024-X](https://doi.org/10.1016/S0889-8529(01)00024-X)
13. Konsman, J. P., Parnet, P., & Dantzer, R. (2002). Cytokine-induced sickness behaviour: mechanisms and implications. *Trends in Neurosciences*, 25(3), 154–159. [https://doi.org/10.1016/S0166-2236\(00\)02088-9](https://doi.org/10.1016/S0166-2236(00)02088-9)
14. Lee, S., Kang, B.-M., Shin, M.-K., Min, J., Heo, C., Lee, Y., ... Suh, M. (2015). Chronic Stress Decreases Cerebrovascular Responses During Rat Hindlimb Electrical Stimulation. *Frontiers in Neuroscience*, 9. <https://doi.org/10.3389/fnins.2015.00462>
15. Kim, Y.-W., West, X. Z., & Byzova, T. v. (2013). Inflammation and oxidative stress in angiogenesis and vascular disease. *Journal of Molecular Medicine*, 91(3), 323–328. <https://doi.org/10.1007/s00109-013-1007-3>



16. Mulvany, M. J., & Halpern, W. (1977). Contractile properties of small arterial resistance vessels in spontaneously hypertensive and normotensive rats. *Circulation Research*, 41(1), 19–26. <https://doi.org/10.1161/01.RES.41.1.19>
17. Qi, L., Zhu, J., Hancock, A. M., Dai, C., Zhang, X., Frostig, R. D., & Chen, Z. (2016). Fully distributed absolute blood flow velocity measurement for middle cerebral arteries using Doppler optical coherence tomography. *Biomedical Optics Express*, 7(2), 601. <https://doi.org/10.1364/BOE.7.000601>
18. Mokhtar, S. S., & Rasool, A. H. G. (2015). Role of endothelium-dependent hyperpolarisation and prostacyclin in diabetes. *The Malaysian journal of medical sciences : MJMS*, 22(2), 8–17.
19. KARAKI, H., URAKAWA, N., & KUTSKY, P. (1984). Potassium-induced contraction in smooth muscle. *Japanese Journal of Smooth Muscle Research*, 20(6), 427–444. <https://doi.org/10.1540/jsmr1965.20.427>
20. Chantler, P. D., Shrader, C. D., Tabone, L. E., d'Audiffret, A. C., Huseynova, K., Brooks, S. D., ... Frisbee, J. C. (2015). Cerebral Cortical Microvascular Rarefaction in Metabolic Syndrome is Dependent on Insulin Resistance and Loss of Nitric Oxide Bioavailability. *Microcirculation*, 22(6), 435–445. <https://doi.org/10.1111/micc.12209>
21. Mariampillai, A., Standish, B. A., Moriyama, E. H., Khurana, M., Munce, N. R., Leung, M. K. K., ... Yang, V. X. D. (2008). Speckle variance detection of microvasculature using swept-source optical coherence tomography. *Optics Letters*, 33(13), 1530. <https://doi.org/10.1364/OL.33.001530>
22. Olfert, I. M., Baum, O., Hellsten, Y., & Egginton, S. (2016). Advances and challenges in skeletal muscle angiogenesis. *American journal of physiology. Heart and circulatory physiology*, 310(3), H326-36. <https://doi.org/10.1152/ajpheart.00635.2015>

23. Sweeney, M. D., Kisler, K., Montagne, A., Toga, A. W., & Zlokovic, B. V. (2018). The role of brain vasculature in neurodegenerative disorders. *Nature Neuroscience*, *21*(10), 1318–1331. <https://doi.org/10.1038/s41593-018-0234-x>
24. Wenceslau, C. F., McCarthy, C. G., Earley, S., England, S. K., Filosa, J. A., Gouloupoulou, S., ... Webb, R. C. (2021). Guidelines for the measurement of vascular function and structure in isolated arteries and veins. *American journal of physiology. Heart and circulatory physiology*, *321*(1), H77–H111. <https://doi.org/10.1152/ajpheart.01021.2020>
25. Pilarczyk, M., Rygula, A., Kaczor, A., Mateuszuk, L., Maślak, E., Chlopicki, S., & Baranska, M. (2014). A novel approach to investigate vascular wall in 3D: Combined Raman spectroscopy and atomic force microscopy for aorta en face imaging. *Vibrational Spectroscopy*, *75*, 39–44. <https://doi.org/https://doi.org/10.1016/j.vibspec.2014.09.004>
26. Bathala, L., Mehndiratta, M. M., & Sharma, V. K. (2013). Cerebrovascular ultrasonography: Technique and common pitfalls. *Annals of Indian Academy of Neurology*, *16*(1), 121–7. <https://doi.org/10.4103/0972-2327.107723>
27. Fantini, S., Sassaroli, A., Tgavalekos, K. T., & Kornbluth, J. (2016). Cerebral blood flow and autoregulation: current measurement techniques and prospects for noninvasive optical methods. *Neurophotonics*, *3*(3), 031411. <https://doi.org/10.1117/1.NPh.3.3.031411>
28. Nelson, A. R., Sweeney, M. D., Sagare, A. P., & Zlokovic, B. V. (2016). Neurovascular dysfunction and neurodegeneration in dementia and Alzheimer's disease. *Biochimica et Biophysica Acta (BBA) - Molecular Basis of Disease*, *1862*(5), 887–900. <https://doi.org/10.1016/j.bbadis.2015.12.016>
29. Zlokovic, B. V. (2011). Neurovascular pathways to neurodegeneration in Alzheimer's disease and other disorders. *Nature Reviews Neuroscience*, *12*(12), 723–738. <https://doi.org/10.1038/nrn3114>

30. Wu, L., Xiong, X., Wu, X., Ye, Y., Jian, Z., Zhi, Z., & Gu, L. (2020). Targeting Oxidative Stress and Inflammation to Prevent Ischemia-Reperfusion Injury. *Frontiers in Molecular Neuroscience*, *13*.  
<https://doi.org/10.3389/fnmol.2020.00028>
31. Grochowski, C., Litak, J., Kamieniak, P., & Maciejewski, R. (2018). Oxidative stress in cerebral small vessel disease. Role of reactive species. *Free Radical Research*, *52*(1), 1–13. <https://doi.org/10.1080/10715762.2017.1402304>
32. Gold, P. W., Machado-Vieira, R., & Pavlatou, M. G. (2015). Clinical and Biochemical Manifestations of Depression: Relation to the Neurobiology of Stress. *Neural Plasticity*, *2015*, 1–11. <https://doi.org/10.1155/2015/581976>
33. Chrissobolis, S. (2011). Oxidative stress and endothelial dysfunction in cerebrovascular disease. *Frontiers in Bioscience*, *16*(1), 1733.  
<https://doi.org/10.2741/3816>
34. Sinha, N., & Dabla, P. (2015). Oxidative Stress and Antioxidants in Hypertension—A Current Review. *Current Hypertension Reviews*, *11*(2), 132–142.  
<https://doi.org/10.2174/1573402111666150529130922>
35. Iuchi, T., Akaike, M., Mitsui, T., Ohshima, Y., Shintani, Y., Azuma, H., & Matsumoto, T. (2003). Glucocorticoid excess induces superoxide production in vascular endothelial cells and elicits vascular endothelial dysfunction. *Circulation research*, *92*(1), 81–7. <https://doi.org/10.1161/01.res.0000050588.35034.3c>
36. Loft, S., & Poulsen, H. E. (1996). Cancer risk and oxidative DNA damage in man. *Journal of Molecular Medicine*, *74*(6), 297–312.  
<https://doi.org/10.1007/BF00207507>
37. Griendling, K. K., Touyz, R. M., Zweier, J. L., Dikalov, S., Chilian, W., Chen, Y.-R., ... American Heart Association Council on Basic Cardiovascular Sciences. (2016). Measurement of Reactive Oxygen Species, Reactive Nitrogen Species, and Redox-Dependent Signaling in the Cardiovascular System: A Scientific Statement

- From the American Heart Association. *Circulation research*, 119(5), e39-75.  
<https://doi.org/10.1161/RES.000000000000110>
38. Johnson, J. D., Barnard, D. F., Kulp, A. C., & Mehta, D. M. (2019). Neuroendocrine Regulation of Brain Cytokines After Psychological Stress. *Journal of the Endocrine Society*, 3(7), 1302–1320.  
<https://doi.org/10.1210/js.2019-00053>
39. Berkowitz, B. A. (2018). Oxidative stress measured in vivo without an exogenous contrast agent using QUEST MRI. *Journal of magnetic resonance (San Diego, Calif. : 1997)*, 291, 94–100. <https://doi.org/10.1016/j.jmr.2018.01.013>
40. Isingrini, E., Surget, A., Belzung, C., Freslon, J.-L., Frisbee, J., O'Donnell, J., ... d'Audiffret, A. (2011). Altered aortic vascular reactivity in the unpredictable chronic mild stress model of depression in mice: UCMS causes relaxation impairment to ACh. *Physiology & behavior*, 103(5), 540–6.  
<https://doi.org/10.1016/j.physbeh.2011.04.002>
41. Pun, P. B. L., Lu, J., & Mochhala, S. (2009). Involvement of ROS in BBB dysfunction. *Free radical research*, 43(4), 348–64.  
<https://doi.org/10.1080/10715760902751902>
42. Scapagnini, G., Davinelli, S., Drago, F., De Lorenzo, A., & Oriani, G. (2012). Antioxidants as antidepressants: fact or fiction? *CNS drugs*, 26(6), 477–90.  
<https://doi.org/10.2165/11633190-000000000-00000>
43. Wallin, A., Blennow, K., Fredman, P., Gottfries, C. G., Karlsson, I., & Svennerholm, L. (2009). Blood brain barrier function in vascular dementia. *Acta Neurologica Scandinavica*, 81(4), 318–322. <https://doi.org/10.1111/j.1600-0404.1990.tb01562.x>
44. Lin, Z., Sur, S., Liu, P., Li, Y., Jiang, D., Hou, X., ... Lu, H. (2021). Blood–Brain Barrier Breakdown in Relationship to Alzheimer and Vascular Disease. *Annals of Neurology*, 90(2), 227–238. <https://doi.org/10.1002/ana.26134>

45. Wu, M.-C., Hsu, J.-L., & Lai, T. W. (2021). Evans blue dye as an indicator of albumin permeability across a brain endothelial cell monolayer in vitro. *Neuroreport*, 32(11), 957–964. <https://doi.org/10.1097/WNR.0000000000001690>
46. Liu, W.-Y., Wang, Z.-B., Zhang, L.-C., Wei, X., & Li, L. (2012). Tight junction in blood-brain barrier: an overview of structure, regulation, and regulator substances. *CNS neuroscience & therapeutics*, 18(8), 609–15. <https://doi.org/10.1111/j.1755-5949.2012.00340.x>
47. Borski, R. J., Hyde, G. N., & Fruchtman, S. (2002). Signal transduction mechanisms mediating rapid, nongenomic effects of cortisol on prolactin release. *Steroids*, 67(6), 539–48. [https://doi.org/10.1016/s0039-128x\(01\)00197-0](https://doi.org/10.1016/s0039-128x(01)00197-0)
48. Zlokovic, B. V. (2011). Neurovascular pathways to neurodegeneration in Alzheimer’s disease and other disorders. *Nature Reviews Neuroscience*, 12(12), 723–738. <https://doi.org/10.1038/nrn3114>
49. Morris, G., Puri, B. K., Olive, L., Carvalho, A., Berk, M., Walder, K., ... Maes, M. (2020). Endothelial dysfunction in neuroprogressive disorders-causes and suggested treatments. *BMC medicine*, 18(1), 305. <https://doi.org/10.1186/s12916-020-01749-w>
50. D’Orléans-Juste, P., Akide Ndunge, O. B., Desbiens, L., Tanowitz, H. B., & Desruisseaux, M. S. (2019). Endothelins in inflammatory neurological diseases. *Pharmacology & therapeutics*, 194, 145–160. <https://doi.org/10.1016/j.pharmthera.2018.10.001>
51. Bajpai, A., Verma, A. K., Srivastava, M., & Srivastava, R. (2014). Oxidative stress and major depression. *Journal of clinical and diagnostic research : JCDR*, 8(12), CC04-7. <https://doi.org/10.7860/JCDR/2014/10258.5292>
52. Milatovic, D., Montine, T. J., & Aschner, M. (2011). Measurement of isoprostanes as markers of oxidative stress. *Methods in molecular biology (Clifton, N.J.)*, 758, 195–204. [https://doi.org/10.1007/978-1-61779-170-3\\_13](https://doi.org/10.1007/978-1-61779-170-3_13)

53. Yoon, C. Y., Steffen, L. M., Gross, M. D., Launer, L. J., Odegaard, A., Reiner, A., ... Jacobs, D. R. (2017). Circulating Cellular Adhesion Molecules and Cognitive Function: The Coronary Artery Risk Development in Young Adults Study. *Frontiers in cardiovascular medicine*, 4, 37. <https://doi.org/10.3389/fcvm.2017.00037>
54. Lin, S.-K., Hsiu, H., Chen, H.-S., & Yang, C.-J. (2021). Classification of patients with Alzheimer's disease using the arterial pulse spectrum and a multilayer-perceptron analysis. *Scientific Reports*, 11(1), 8882. <https://doi.org/10.1038/s41598-021-87903-7>
55. Wang, S., Tang, C., Liu, Y., Border, J. J., Roman, R. J., & Fan, F. (2022). Impact of impaired cerebral blood flow autoregulation on cognitive impairment. *Frontiers in Aging*, 3. <https://doi.org/10.3389/fragi.2022.1077302>
56. Meissner, A. (2016). Hypertension and the Brain: A Risk Factor for More Than Heart Disease. *Cerebrovascular Diseases*, 42(3–4), 255–262. <https://doi.org/10.1159/000446082>
57. Girouard, H., & Iadecola, C. (2006). Neurovascular coupling in the normal brain and in hypertension, stroke, and Alzheimer disease. *Journal of Applied Physiology*, 100(1), 328–335. <https://doi.org/10.1152/jappphysiol.00966.2005>
58. Falvo, M. J., Lindheimer, J. B., & Serrador, J. M. (2018). Dynamic cerebral autoregulation is impaired in Veterans with Gulf War Illness: A case-control study. *PLOS ONE*, 13(10), e0205393. <https://doi.org/10.1371/journal.pone.0205393>
59. Sutherland, B. A., Rabie, T., & Buchan, A. M. (2014). Laser Doppler flowmetry to measure changes in cerebral blood flow. *Methods in molecular biology (Clifton, N.J.)*, 1135, 237–48. [https://doi.org/10.1007/978-1-4939-0320-7\\_20](https://doi.org/10.1007/978-1-4939-0320-7_20)

## Chapter 2

### 2 Integrated Article 1: A novel vascular health index: Using data analytics and population health to facilitate mechanistic modeling of microvascular status

#### 2.1 Introduction

The study of vascular function under control or “healthy” conditions has been an intensive area of investigation across the translational research spectrum for many years. Operating in parallel have been investigations into how the defining parameters and integrated systems of vascular function are modified with the development of states of elevated disease risk or outright disease itself [1; 2], healthy aging [3], or a variety of imposed experimental conditions (e.g., physical inactivity [4], traumatic injury [5], etc.). While these diverse efforts have provided us with a broad perspective for what constitutes vascular health and dysfunction, it has also created challenges for our ability to compare and integrate results across numerous research groups, animal models, and experimental conditions. Specifically, we continue to struggle with our ability to move from correlative measures and predictive biomarkers of vascular dysfunction to an understanding of integrated vascular function within the larger context of health and disease. Beyond gaining insight into markers of dysfunction and how they may frame our understanding of the impact of disease and elevated disease risk, it is increasingly important for us to be able to place the experimental results and datasets from different models of vasculopathy risk onto an appropriate spectrum of function. The general question to be considered is “how dysfunctional is the vasculature compared to ideal or to other compromised conditions?”.

When we consider the issues of developing an integrated perspective of vascular dysfunction, we encounter two categories of conceptual challenges: data-independent issues (i.e., comparability issues across models, research groups, and experimental approaches) and data-dependent issues (i.e., issues related to database content, statistical and analytical constraints, etc.). From the perspective of data-independency, we must consider conceptual challenges from a physiological perspective; specifically, how to define and quantify “vascular function” across a spectrum of conditions. This can include relative contributions of mediators of vascular function, the relative importance of these contributors in the spatial and temporal regulation of tissue perfusion, and even the targeting of interventions to achieve prodromic or postdromic prevention in specific conditions. Further, heterogeneity in models and approaches used must be considered such that differences between experimental designs undertaken by different research groups can be effectively compared.

From the perspective of data-dependency, there are several practical and technical challenges facing basic scientists from the perspectives of comparing datasets between conditions and research groups. These can include small sample sizes (as compared to population science or clinical cohort studies) and complex study designs that include highly specialized preparations, protocols or treatment regimes designed to address very specific research questions or hypotheses. For any given study, while a tremendous number of variables may be collected or generated, the traditional basic science paradigm typically limits the use of these data beyond their original intent, prohibiting the pooling or combining of data from different studies at different time points to address emerging questions. Consequently, the advances, insights, and knowledge realized in clinical and



population research settings have not been realized by the basic sciences. This can include techniques and approaches from artificial intelligence/machine learning, “big data” techniques, and metanalyses, and linkage of datasets and sources across data types and time, from imaging data to electronic medical records to social services to birth registries and tissue banks. Additionally, basic sciences are further limited because there are no “secondary sources” of animal data that scientists can readily access – all data is, by necessity, primary data and each experiment can cost many thousands of dollars depending upon the animal model and specific performed procedures.

To realize the comparable benefits that data science has afforded the human subject and clinical research realms of the translational spectrum, basic scientists must develop approaches and tools that will allow them to consolidate data from multiple primary studies, collected at different levels of spatial and temporal resolution and across diverse experimental protocols. Further, they must also be able to consolidate many high-resolution data points into more encompassing constructs of “health”, “dysfunction”, or “disease” that allow for broader comparability. A goal is to transition from empirical evaluations of pathways and mechanisms toward a more complex analysis of integrated, holistic mechanistic models. In this manuscript, we describe an approach to establish and validate an integrated, composite metric that quantifies vascular dysfunction in elevated peripheral vascular disease (PVD) and cerebrovascular disease (CeVD) risk states as compared to vascular function in healthy, age-matched, control conditions. Once developed and validated, this metric can be used in mechanistic modeling to gain greater insight into the temporal and spatial development of vascular dysfunction within the context of physiological and pathophysiological systems. Finally, it is anticipated that the

general approach to the development of such an index could be applied by other research groups to achieve similar goals in transitioning to more integrated, holistic mechanistic models. The primary objectives of this study are to develop an integrated vascular health index (VHI) for both the skeletal muscle and cerebral circulations and report on the presentation and validity of the metric.

## 2.2 Materials and Methods

Much of the data in the present manuscript have been published previously and these citations will be made at the appropriate points in the text. However, this manuscript represents the inclusion of both *de novo* experiments and analyses, previously unpublished results and analyses, and the pooling of data from previous studies for novel analyses. The present study serves as part of a larger goal of gaining additional insights from data collected from previous experiments and peer-reviewed, published studies by utilizing data science and more sophisticated analytic approaches, and mechanistic modeling. The protocols and specific methodology for the collection of the specific vascular phenotypes and the subsequent calculation of a Vascular Health Index (VHI) are summarized and fully referenced below.

### 2.2.1 Animal Model

All experiments and analyses described in this manuscript utilized male lean (LZR) and obese (OZR) Zucker rats. Animals were purchased from the supplier (Harlan/Envigo) at 6-7 weeks of age and were housed in an accredited animal care facility at the Medical College of Wisconsin, West Virginia University, or the University of Western Ontario, with *ad libitum* access to normal chow and water until the time of final usage unless

otherwise noted. Following one week of acclimation, rats were placed into one of three groups until their final usage:

1. Time control (LZR and OZR were housed without intervention and aged to a maximum of ~20 weeks)
2. Treadmill exercise (20 m/min, 5% incline, 60 minutes/day, 6 days/week; [6])
3. Captopril (angiotensin converting enzyme inhibitor captopril ( $60 \text{ mg}\cdot\text{kg}^{-1}\cdot\text{day}^{-1}$ ); mixed with food [7])

At the time of final usage, each rat was deeply anesthetized with sodium pentobarbital ( $50 \text{ mg}\cdot\text{kg}^{-1}$  i.p.) and the trachea was intubated to maintain a patent airway. In all rats, a carotid artery and an external jugular vein were cannulated to measure arterial pressure and to infuse additional anesthetic, respectively, as necessary. At this time, an aliquot of blood was drawn from the jugular vein of each animal to be used for the subsequent determination of plasma metabolic/endocrine, oxidant stress, and inflammatory biomarker profiles using commercially available kits ([7]). All procedures followed approved IACUC protocols at each institution.

***Evaluation of Vascular Reactivity:*** The assessment of arteriolar reactivity from skeletal muscle was determined using the intramuscular continuation of the gracilis arteries, which were removed from each leg following the procedures in the neck (above). Subsequently, the rat was given a lethal overdose of pentobarbital anesthetic, followed by the removal of the head via decapitation. For the assessment of cerebrovascular reactivity, the middle cerebral arteries (MCA) were removed from their origin on the Circle of Willis following the removal of the brain from the skull. Both the gracilis muscle arterioles and the MCAs were doubly-cannulated and placed in a heated chamber ( $37^\circ\text{C}$ ) that allowed the vessel

lumen and exterior to be perfused and superfused, respectively, with physiological salt solution (PSS; equilibrated with 21% O<sub>2</sub>, 5% CO<sub>2</sub>; 74% N<sub>2</sub>) from separate reservoirs [8; 9]. Vessel diameter was measured using television microscopy and an on-screen video micrometer. Both vessels were extended to their *in situ* length and were equilibrated at 80% of the animal's mean arterial pressure [8; 9].

In both gracilis muscle arterioles and MCAs, vascular reactivity was evaluated in response to application of acetylcholine (10<sup>-9</sup> M – 10<sup>-6</sup> M) and sodium nitroprusside (10<sup>-9</sup> M – 10<sup>-6</sup> M). In addition, the reactivity of isolated MCAs and gracilis muscle arterioles was assessed following hypoxic challenge with reduced PO<sub>2</sub> ( $\Delta$ PO<sub>2</sub> from ~135 mmHg [21% O<sub>2</sub>] – ~45 mmHg [0% O<sub>2</sub>]) to assess endothelial function and dilator responses [10].

The mechanical responses of isolated arterioles following pharmacological challenge with any of the agonists were fit with the following logistic equation:

$$y = \min + \left[ \frac{\max - \min}{1 + 10^{\log EC_{50} - x}} \right]$$

where  $y$  represents the change in arteriolar diameter, “min” and “max” represent the lower and upper bounds, respectively, of the change in arteriolar diameter with increasing agonist concentration,  $x$  is the logarithm of the agonist concentration and  $\log EC_{50}$  represents the logarithm of the agonist concentration ( $x$ ) at which the response ( $y$ ) is halfway between the lower and upper bounds.

***Evaluation of Vascular Wall Mechanics:*** Following the experimental procedures for measuring *ex vivo* vascular reactivity for both MCA and gracilis arterioles, the perfusate

and superfusate PSS were replaced with  $\text{Ca}^{2+}$ -free PSS containing the metal ion chelators EDTA (0.03mM) and EGTA (2.0mM). Vessels were challenged with  $10^{-7}$  M phenylephrine (gracilis arterioles) or serotonin (middle cerebral arteries) until all active tone was lost. Subsequently, intraluminal pressure within the isolated vessel was altered, in 20 mmHg increments, between 0 mmHg and 160 mmHg. To ensure that a negative intraluminal pressure was not exerted on the vessel, 5 mmHg was used as the “0 mmHg” intraluminal pressure point; all other values of intraluminal pressure were multiples of 20 mmHg up to 160 mmHg. After 5-7 minutes at each intraluminal pressure, the inner and outer diameter of the isolated vessel was determined.

All calculations of passive arteriolar wall mechanics (used as indicators of structural alterations to the individual microvessel) are based on those used previously [11; 12]. Vessel wall thickness was calculated as:

$$WT = \frac{(OD - ID)}{2}$$

where  $WT$  represents wall thickness ( $\mu\text{m}$ ) and  $OD$  and  $ID$  represent arteriolar outer and inner diameter, respectively ( $\mu\text{m}$ ).

For the calculation of circumferential stress, intraluminal pressure was converted from mmHg to  $\text{N}/\text{m}^2$ , where  $1 \text{ mmHg} = 1.334 \times 10^2 \text{ N}/\text{m}^2$ . Circumferential stress ( $\sigma$ ) was then calculated as:

$$\sigma = \frac{(P_{IL} \times ID)}{(2WT)}$$

where  $P_{IL}$  represents the intraluminal pressure. Circumferential strain ( $\varepsilon$ ) was calculated as:

$$\varepsilon = \frac{(ID - ID_5)}{ID_5}$$

where  $ID_5$  represents the internal arteriolar diameter at the lowest intraluminal pressure (i.e., 5 mmHg). The stress versus strain relationship from each vessel was fit (ordinary least squares analyses,  $r^2 > 0.85$ ) with the following exponential equation:

$$\sigma = \sigma_5 e^{\beta\varepsilon}$$

where  $\sigma_5$  represents circumferential stress at  $ID_5$  and  $\beta$  is the slope coefficient describing arterial stiffness. Higher levels of  $\beta$  are indicative of increasing arterial stiffness (i.e., requiring a greater degree of distending pressure to achieve a given level of wall deformation; [11; 13]).

***Histological Determination of Skeletal Muscle Microvessel Density:*** At the conclusion of the muscle contraction protocols, the gastrocnemius muscle was removed, rinsed in PSS and fixed in 0.25% formalin. Muscles were embedded in paraffin and cut into 5  $\mu\text{m}$  cross sections. Sections were incubated with *Griffonia simplicifolia* I lectin (a general microvessel stain for all vessels  $< 20 \mu\text{m}$  diameter), as described previously [14; 15]. After exposure to lectin, sections were rinsed three times in PSS and were mounted on microscope slides with a water-soluble mounting medium (SP, ACCU-MOUNT 280, Baxter). Using epifluorescence microscopy, localization of labeled microvessels was performed with a Nikon E600 upright microscope with a 20x objective lens (Plan Fluo

phase NA 0.5). Excitation was provided by a 75 watt Xenon Arc lamp through a Lambda 10-2 optical filter changer (Sutter Instrument Company, Novato, CA) controlling a 595nm excitation filter and a 615 nm emission filter. The microscope was coupled to cooled CCD camera (Micromax; Princeton Instruments Inc, Trenton, NJ). From each gastrocnemius muscle, six individual cross sections were used for analysis, with six randomly selected regions within an individual cross section chosen for study and each region of study had an area of  $\sim 1.47 \times 10^5 \mu\text{m}^2$  [16; 17]. All acquired images from individual sections were analyzed for number of microvessels and number of skeletal muscle fibers using MetaMorph Imaging software (Universal Imaging Co., Downingtown, PA).

***Determination of Cerebral Cortex Microvessel Density:*** Following removal of the MCAs from the Circle of Willis on the base of the brain, the brain was placed within Tissue-Tek OCT compound and frozen. Brains were then sliced into 5  $\mu\text{m}$  cross sections and were then stained using the established approach developed by Munzenmaier and Greene [18] using primary anti-CD-31 antibody. Under microscopy, localization of labeled microvessels was performed with a Nikon E600 upright microscope with a 20x objective lens [19]. The microscope was coupled to cooled CCD camera (Micromax; Princeton Instruments Inc, Trenton, NJ). Five nearby 1  $\text{mm}^2$  images were taken from each of three sections in the frontal cortex of each brain, and the mean microvessel density within these 15 images was taken to represent cortical MVD in that animal. All acquired images from individual sections were analyzed for number of microvessels using MetaMorph Imaging software (Universal Imaging Co., Downingtown, PA).[19]

## 2.2.2 Development of vascular health index (VHI)

*Determination of VHI characteristics:* In developing the VHI and ensuring it can effectively capture critical aspects of vascular structure and function, the following considerations were made:

- 1) Given the many structural and functional differences between the cerebral and peripheral vasculature, a metric representing the health of their vasculature must be calibrated and calculated separately to yield a cerebral VHI and a peripheral VHI.
- 2) The metric must be a composite measure that accounts for distinct aspects of vascular function and structure, such as vessel reactivity, vascular wall mechanics, and network characteristics.
- 3) The metric will not be a predictive measure but instead will describe the relative state of the vasculature at a given time. Given this, there is no basis for establishing parameter weighting or coefficients for the different components within the composite metric. That is, all components are weighted equally.
- 4) The use and calculation of such a metric needs to be practical and feasible insofar that the components of the metric need to be relatively easily collected in sufficient frequency to facilitate the actual quantitative determination of the metric in significant amounts, not just for our research group but other interested research teams as well. [11]
- 5) Given that the validity of a metric is the degree to which values from that metric represent the variable they intend to, we will need several forms of evidence to establish VHI as a valid estimator of vascular health. The specific forms of evidence/aspects of validity of concern are:



- a) **Face validity [20]:** the extent to which a metric appears to measure the construct of interest; are the parameters used in the development of the metric appropriate to the intention?
- b) **Content Validity [20]:** determines whether the index is appropriately representative of the aspects of the system being modeled. Does the content of the metric encompass the relevant aspects it is intended to estimate?
- c) **Criterion Validity [20]:** the extent to which the index responds in a manner that is consistent with general understanding and developed hypotheses and represents how well the value of the metric is indicative of the underlying theory of the system. Specifically, it is the extent to which values of a metric are correlated with other criterion variables that one would expect the measure to be correlated with.
- d) **Discriminant Validity [20]:** this determines the ability of the metric to distinguish between populations with differing levels of the underlying construct (vascular health). For example, our metric must be able to distinguish a population of obese Zucker rats from their lean counterparts as well as any effective treatment group that works to mitigate or minimize vascular dysfunction (like a population of obese Zucker rats under an exercise or drug regimen).

In evaluating the above criteria, we have developed a 3-component and 5-component version of both a cerebral VHI and peripheral VHI in Zucker rats. The rationale is that, for many of the data pooling opportunities across time and research groups, the use of a 3-

component metric (composed of commonly collected measures) would allow for much larger sample sizes while still capturing the essential aspects of vascular health.

***VHI Parameter Selection:*** Three fundamental aspects of healthy vasculature are the ability of resistance vessels to respond appropriately to vasoactive stimuli, the mechanics (i.e., the distensibility or stiffness) of the arteriolar wall, and the structure of the microvascular network from the perspective of a microvessel/capillary density within perfused tissue. Thus, to ensure face validity as well as content validity, the components of the VHI were selected to represent these differing major descriptors of vascular health. For the 3-component VHI, vascular responses to acetylcholine (reactivity), the slope ( $\beta$ ) coefficient from the vascular wall stress versus strain relation (wall mechanics) and tissue microvessel density (network structure) were selected. For the 5-component VHI, these same parameters were used with the additional inclusion of two markers of vascular reactivity: the responses to sodium nitroprusside and to hypoxia.

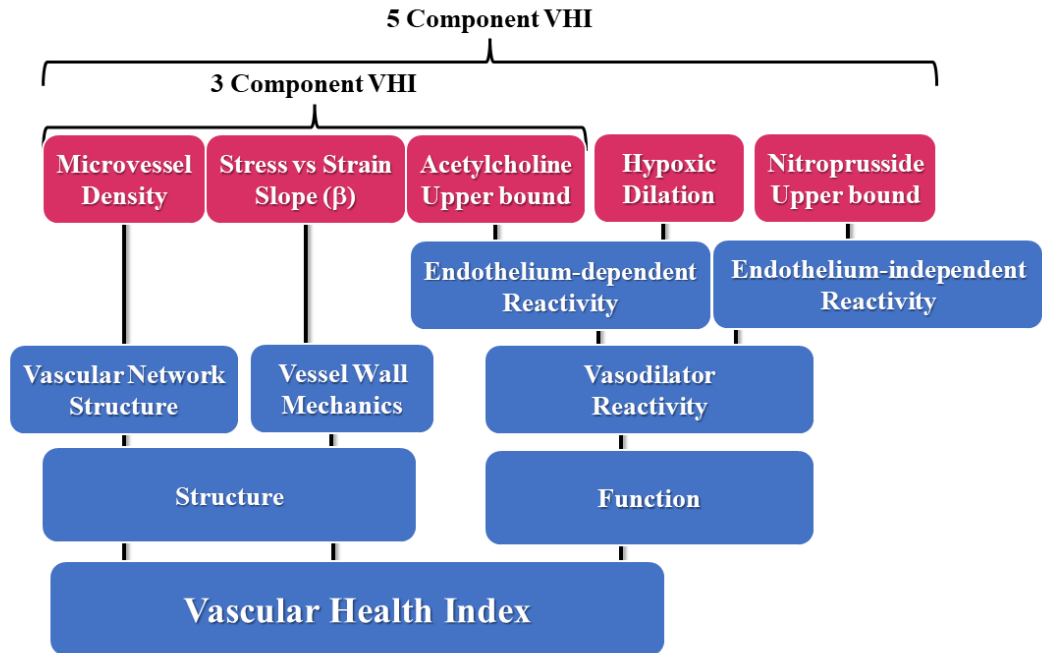


**Figure 2-1: Schematic representation of the VHI components**

Figure 2-1: Schematic representation of the components contributing to the 5- and 3-parameter calculations for the Vascular Health Index (VHI), and their context within the scope of vascular structure and function.

***Assessing the Four Aspects of Validity:***

***Face Validity:*** Being the weakest and least rigorous form of validity, face validity is often assessed informally. For our purposes with VHI, the assessment was made in the process of parameter selection for the components of the measure. This is represented in Figure 1, where the conceptual design summarizes the major aspects of vascular function used in the present study, where each of the domains are represented in the calculations of VHI.

**Content Validity:** The content validity of the measure was ensured by clearly defining and restricting the components of “vascular health” to three major aspects and appropriately representing those aspects in the VHI. The three main aspects of vascular health are the reactivity of resistance vessels, arteriolar wall mechanics, and microvessel density within the tissue.

**Criterion Validity:** In assessing criterion validity we need to identify a variable with which we would expect individual values of VHI in a given population to be correlated. For the present study, both plasma insulin and TNF- $\alpha$  concentrations were selected as the criterion with an expected correlation to VHI in a population of obese Zucker rats. To demonstrate criterion validity there needs to be a significant correlation between the insulin and TNF- $\alpha$  concentrations and the VHI of obese Zucker rats aged 7 weeks to 20 weeks.

**Discriminant Validity:** We will demonstrate the metric’s discriminant validity by distinguishing specific populations of Zucker rats using only their VHI values; specifically, populations of obese Zucker rats, obese Zucker rats that underwent a regular exercise regimen, obese Zucker rats that have been treated with an anti-hypertensive ACE inhibitor (captopril), and lean Zucker rats.

**Construction of the measure:** In constructing VHI and its calculation, the following general principles were used:

1. The metric will be calculated at different age points (7, 10, 13, 15, 17, and 20 weeks old); meaning comparisons are done between lean and obese Zucker rats across

ages of the animal and the resultant composite score can be considered independent of the specific age of the animals.

2. With the “ideal” vascular health quantified in control rats, an animal experiencing an altered condition from this (e.g., elevated disease risk, interventional treatments, etc.) can then be quantitatively compared to this ideal standard of health. The simplest way to do this is to calculate a percentage-based score, where the measurement for the sick animal is expressed as a percentage (%) of the value for the age-matched healthy standard. Thus, the metric is interpreted as % of ideal vascular health.
3. A single parameter, the VHI, is then calculated by averaging the component score (a percentage of ideal) across all 3 or 5 components in the index. This is repeated for both the cerebral and peripheral index. To calculate the index in control (i.e., healthy, untreated) animals the calculations were performed as outlined in Table 1. It should be noted that, with both age and disease risk, some variables are expected to increase as animals (e.g., vascular wall stiffness) become unhealthy whereas others decrease (e.g., endothelial function). This has been addressed in the calculations for the vascular wall stiffness component score by treating the relative increase above the associated standard of health value as a corresponding deficit to the component score (%).
4. The metric will be a measure of “health”, where healthy animals (male, lean, untreated Zucker rats) that served as control animals in previous studies were used to define ideal vascular function (ideal standards for each component of VHI) at different age points. Therefore, the VHI of a given rat will represent any unhealthy

deviation in the health of its vasculature. Given the use of data across multiple studies, the VHI of any age matched rat under an experimental condition will be calculated relative to the specific control (male, untreated lean Zucker rats) values of the original experiment.

**Table 2-1: Calculations of VHI Components**

<b>Component</b>	<b>Expected Deviation from LZR with Disease Risk</b>	<b>Formula used to Calculate VHI Component</b>
Acetylcholine-induced Dilation (upper bound; $\mu\text{m}$ )	Reduced ( $\downarrow$ )	$\frac{\textit{Measurement}}{\textit{Standard of health}} \times 100$
Microvessel Density ( $\#/\text{mm}^2$ )	Reduced ( $\downarrow$ )	$\frac{\textit{Measurement}}{\textit{Standard of health}} \times 100$
Circumferential Stress vs Strain Slope Coefficient ( $\beta$ )	Increased ( $\uparrow$ )	$100 + \left( 100 - \left[ \frac{\textit{Measurement}}{\textit{Standard of health}} \times 100 \right] \right)$
Sodium Nitroprusside-induced Dilation (upper bound; $\mu\text{m}$ )	Reduced ( $\downarrow$ )	$\frac{\textit{Measurement}}{\textit{Standard of health}} \times 100$
Hypoxic Dilation ( $\mu\text{m}$ )	Reduced ( $\downarrow$ )	$\frac{\textit{Measurement}}{\textit{Standard of health}} \times 100$

## 2.3 Results

Table 2 summarizes the samples sizes of all animal groups, at all ages, used in the present study. The baseline characteristics of the animals used in the present study, at each age, are summarized in Table 3. Tables 4 and 5 present the raw data describing the different VHI components used in the present study for the peripheral (skeletal muscle) and cerebral vasculature, respectively. The aggregate values of skeletal muscle and cerebral VHI are summarized in Table 6.

**Table 2-2: Sample sizes of present study**

Animal numbers used in the present study. Data are presented for each group of animals and at each age for both the peripheral and cerebral vascular health index (VHI) calculations.

<b>Animal Group</b>	<b>Age (Weeks)</b>	<b>Peripheral VHI ‘n’</b>		<b>Cerebral VHI ‘n’</b>	
		<b>5 Component</b>	<b>3 Component</b>	<b>5 Component</b>	<b>3 Component</b>
<b>OZR</b>	<b>7</b>	16	36	8	20
	<b>10</b>	16	30	8	8
	<b>13</b>	16	36	8	14
	<b>17</b>	28	28	8	12

	<b>20</b>	0	6	8	8
	<b>Total</b>	<b>76</b>	<b>136</b>	<b>40</b>	<b>62</b>
<b>OZR + Exercise</b>	<b>7</b>	7	7	-	-
	<b>10</b>	7	7	-	-
	<b>13</b>	7	7	-	-
	<b>17</b>	7	23	-	-
	<b>20</b>	-	-	-	-
	<b>Total</b>	<b>28</b>	<b>44</b>	-	-
<b>OZR + Captopril</b>	<b>7</b>	4	4	-	6
	<b>10</b>	4	4	-	-
	<b>13</b>	4	4	-	6
	<b>17</b>	4	4	-	6
	<b>20</b>	-	-	-	-
	<b>Total</b>	<b>16</b>	<b>16</b>	-	<b>18</b>
<b>LZR</b>	<b>7</b>	25	37	10	22
	<b>10</b>	23	29	10	10
	<b>13</b>	24	36	10	16
	<b>17</b>	22	42	10	12
	<b>20</b>	-	6	11	11



	<b>Total</b>	<b>94</b>	<b>150</b>	<b>51</b>	<b>71</b>
--	--------------	-----------	------------	-----------	-----------

**Table 2-3: Animal baseline characteristics**

Baseline characteristics of animals used in the present study. \* p<0.05 vs. LZR at that age;

† p<0.05 vs. OZR at that age.

<b>Variable</b>	<b>Group</b>	<b>7 wk</b>	<b>10 wk</b>	<b>13 wk</b>	<b>17 wk</b>	<b>20 wk</b>
<b>Mass (g)</b>	<b>LZR</b>	149.7±1.5†	243.0±2.1†	307.2±2.0†	357.5±1.5†	374.3±2.6†
	<b>OZR</b>	233.9±1.8*	409.4±2.6*	512.3±3.2*	682.3±2.5*	741.8±11.0 *
	<b>OZR- Exer</b>	187.3±27.2*†	291.3±29.7 *†	359.3±41.1 *†	441.0±53.3 *†	-
	<b>OZR-Cap</b>	239.0±2.7*	409.0±4.5*	515.3±4.6*	624.3±8.6*	-
<b>Insulin (ng/ml)</b>	<b>LZR</b>	1.0±0.1†	1.2±0.1†	1.3±0.1†	1.1±0.1†	1.5±0.1†
	<b>OZR</b>	3.5±0.1*	5.0±0.1*	7.6±0.2*	7.8±0.1*	10.8±0.6*
	<b>OZR- Exer</b>	1.7±0.4*†	2.4±0.8*†	3.6±1.5*†	4.3±1.9*†	-
	<b>OZR-Cap</b>	3.5±0.2*	3.7±0.3*†	5.4±0.3*†	6.7±0.2*†	-
<b>Glucose (mg/dL)</b>	<b>LZR</b>	93.7±1.1†	98.4±1.1†	100.9±1.1†	100.2±1.4†	104.7±2.0†
	<b>OZR</b>	99.7±1.4*	118.6±3.4*	138.6±2.7*	179.1±1.2*	182.6±2.7*
	<b>OZR- Exer</b>	93.5±5.4	94.0±5.0†	105.0±6.6†	119.0±12.1 *†	-

	<b>OZR-Cap</b>	99.0±3.5*	100.0±2.5†	123.5±2.5* †	137.5±5.3* †	-
<b>N-tyr (ng/dL)</b>	<b>LZR</b>	9.2±0.3†	10.4±0.3†	12.8±0.3†	16.5±0.6†	18.2±1.0†
	<b>OZR</b>	15.0±0.4*	24.8±0.4*	45.4±1.1*	51.7±0.9*	59.6±1.0*
	<b>OZR- Exer</b>	10.3±0.7†	11.8±1.3†	19.0±4.7*†	20.5±6.3*†	-
	<b>OZR-Cap</b>	13.0±0.6*†	16.0±0.7*†	24.5±0.3*†	34.0±0.9*†	-
<b>TNF-<math>\alpha</math> (pg/mL)</b>	<b>LZR</b>	1.7±0.1†	2.0±0.1†	2.4±0.2†	2.2±0.1†	2.6±0.2†
	<b>OZR</b>	4.5±0.2*	8.6±0.3*	10.9±0.2*	8.1±0.3*	13.3±0.4*
	<b>OZR- Exer</b>	1.8±0.3†	2.8±0.8†	3.3±1.0*†	3.5±1.2*†	-
	<b>OZR-Cap</b>	3.5±0.3*†	6.5±0.7*†	7.0±0.9*†	9.5±0.7*†	-

**Table 2-4: Peripheral (skeletal muscle) vascular component data**

<b>Component</b>	<b>Group</b>	<b>7 wk</b>	<b>10 wk</b>	<b>13 wk</b>	<b>17 wk</b>	<b>20 wk</b>
<b>Acetylcholine Dilation (<math>\mu\text{m}</math>)</b>	LZR	119.2 $\pm$ 1.1	125.0 $\pm$ 1.1 $\dagger$	129.3 $\pm$ 1.2 $\dagger$	136.5 $\pm$ 2.0 $\dagger$	139.9 $\pm$ 1.6 $\dagger$
	OZR	115.3 $\pm$ 1.9	118.4 $\pm$ 3.2*	120.5 $\pm$ 2.8*	122.6 $\pm$ 2.9*	119.3 $\pm$ 3.3*
	OZR-Exer	117.6 $\pm$ 2.6	127.3 $\pm$ 2.2 $\dagger$	131.7 $\pm$ 2.3 $\dagger$	129.6 $\pm$ 3.4*	-
	OZR-Cap	118.3 $\pm$ 2.7	117.0 $\pm$ 2.1*	124.8 $\pm$ 3.9	124.3 $\pm$ 1.9*	-
<b>Nitroprussid e Dilation (<math>\mu\text{m}</math>)</b>	LZR	128.8 $\pm$ 0.9	130.6 $\pm$ 1.0	132.9 $\pm$ 1.2	140.3 $\pm$ 2.2	140.7 $\pm$ 1.4
	OZR	127.7 $\pm$ 2.2	131.5 $\pm$ 3.3	134.1 $\pm$ 2.6	139.8 $\pm$ 3.7	135.6 $\pm$ 4.8
	OZR-Exer	127.0 $\pm$ 2.7	132.0 $\pm$ 1.8	135.7 $\pm$ 2.3	134.4 $\pm$ 3.8	-
	OZR-Cap	130.8 $\pm$ 3.2	134.3 $\pm$ 1.5*	138.5 $\pm$ 3.4*	134.0 $\pm$ 2.6*	-
<b>Microvessel Density (#/mm<sup>2</sup>)</b>	LZR	809.9 $\pm$ 13.9	810.4 $\pm$ 13.1	811.8 $\pm$ 11.9 $\dagger$	863.1 $\pm$ 4.6 $\dagger$	823.0 $\pm$ 9.1 $\dagger$
	OZR	805.4 $\pm$ 25.2	782.4 $\pm$ 26.1	706.9 $\pm$ 16.9*	656.3 $\pm$ 20.5*	635.9 $\pm$ 11.6*
	OZR-Exer	881.4 $\pm$ 10.8* $\dagger$	874.6 $\pm$ 14.6* $\dagger$	832.3 $\pm$ 21.5 $\dagger$	869.4 $\pm$ 17.3 $\dagger$	-
	OZR-Cap	833.3 $\pm$ 12.3	813.3 $\pm$ 5.5	764.0 $\pm$ 8.0* $\dagger$	730.5 $\pm$ 16.6* $\dagger$	-
<b>Hypoxic Dilation (<math>\mu\text{m}</math>)</b>	LZR	120.8 $\pm$ 1.1	125.0 $\pm$ 1.0 $\dagger$	128.9 $\pm$ 1.2 $\dagger$	135.3 $\pm$ 1.8 $\dagger$	135.8 $\pm$ 2.0 $\dagger$
	OZR	117.0 $\pm$ 2.2	118.1 $\pm$ 3.1*	119.6 $\pm$ 3.1*	121.6 $\pm$ 4.1*	118.4 $\pm$ 2.1*
	OZR-Exer	121.1 $\pm$ 2.3	126.6 $\pm$ 2.3 $\dagger$	129.6 $\pm$ 2.5 $\dagger$	125.6 $\pm$ 4.8*	-

	OZR-Cap	119.5±3.0	119.5±2.3*	126.8±3.2†	123.0±4.0*	-
<b>Stress vs Strain β</b>	LZR	2.6±0.1	2.6±0.1†	2.8±0.1†	3.1±0.1†	3.2±0.1†
	OZR	2.4±0.3	3.4±0.5*	4.1±0.6*	6.2±0.4*	5.7±0.7*
	OZR-Exer	3.7±0.3*	3.5±0.3*	3.8±0.4*	4.0±0.3*†	-
	OZR-Cap	3.2±0.2*	3.5±0.3*	4.2±0.2*	4.8±0.3*†	-

*Vascular component data, presented as mean±SE, for the animal groups of the present study across all age. \* p<0.05 vs. LZR at that age; † p<0.05 vs. OZR at that age*

**Table 2-5: Cerebral vascular component data**

Data presented as mean±SE, for the animal groups of the present study across all age. \* p<0.05 vs. LZR at that age; † p<0.05 vs. OZR at that age

Component	Group	7 wk	10 wk	13 wk	17 wk	20 wk
<b>Acetylcholine Dilation</b>	LZR	135.2±1.3†	144.1±0.9†	151.8±0.8†	155.0±1.4†	163.0±1.1†
	OZR	122.4±1.3*	128.4±1.0*	125.1±0.8*	122.9±1.7*	119.8±2.5*
	OZR-Exer	-	-	-	-	-
	OZR-Cap	137.5±0.7	-	139.0±0.7*	132.5±2.4*	-
<b>Nitroprusside Dilation</b>	LZR	142.7±1.2†	151.4±0.6†	159.1±1.2†	158.6±1.1†	163.4±1.1†
	OZR	131.1±1.5*	135.3±1.5*	142.1±1.3*	139.8±1.5*	138.5±2.1*
	OZR-Exer	-	-	-	-	-
	OZR-Cap	-	-	-	-	-
<b>Microvessel Density</b>	LZR	290.0±1.9†	293.0±2.1†	303.8±1.2†	313.6±1.4†	319.6±1.0†
	OZR	274.0±3.2*	270.1±2.6*	255.8±2.6*	249.1±2.1*	242.0±1.9*
	OZR-Exer	-	-	-	-	-
	OZR-Cap	337.3±2.7*†	-	332.0±1.7*†	310.3±2.2†	-
<b>Hypoxic Dilation</b>	LZR	132.1±1.2†	140.2±0.7†	149.5±0.9†	152.6±1.5†	159.8±0.9†
	OZR	122.6±1.6*	129.1±1.0*	127.1±0.8*	123.5±1.1*	120.6±2.4*
	OZR-Exer	-	-	-	-	-
	OZR-Cap	-	-	-	-	-
<b>Stress vs Strain <math>\beta</math></b>	LZR	1.6±0.1	1.7±0.1†	1.8±0.1†	2.0±0.1†	2.2±0.1†
	OZR	1.8±0.1	2.1±0.1*	2.8±0.2*	4.0±0.2*	5.4±0.1*

	OZR-Exer	-	-	-	-	-
	OZR-Cap	2.5±0.1*†	-	3.3±0.1*†	4.7±0.1*†	-

**Table 2-6: Calculated vascular health index (VHI)**

(VHI) for each group of animals at each age within the present study. \*  $p < 0.05$  vs. LZR at that age; †  $p < 0.05$  vs. OZR at that age

Animal Group	Age (Weeks)	Peripheral VHI 'n'		Cerebral VHI 'n'	
		5 Component	3 Component	5 Component	3 Component
OZR	7	101.5 ± 1.0	100.8 ± 1.2	91.3 ± 1.1*	92.8 ± 0.8*
	10	92.7 ± 1.7*	88.3 ± 1.9*	87.8 ± 0.8*	85.9 ± 1.2*
	13	86.6 ± 2.1*	79.6 ± 2.2*	76.6 ± 1.6*	75.4 ± 2.4*
	17	70.2 ± 0.9*	63.4 ± 1.3*	64.7 ± 1.8*	60.1 ± 3.1*
	20	-	42.2 ± 1.6*	52.0 ± 1.3*	33.2 ± 2.4*
	Mean	84.2 ± 1.3*	82.2 ± 1.6*	74.5 ± 2.4*	71.4 ± 2.7*
OZR + Exercise	7	97.2 ± 1.9	93.5 ± 3.1†	-	-
	10	97.1 ± 2.9	94.3 ± 4.6	-	-
	13	94.8 ± 4.1†	90.9 ± 5.7*†	-	-
	17	94.8 ± 3.7*†	86.3 ± 3.4*†	-	-
	20	-	-	-	-

	<b>Mean</b>	$95.9 \pm 1.6^{*\dagger}$	$89.7 \pm 2.9^{*\dagger}$	-	-
<b>OZR + Captopril</b>	<b>7</b>	$99.9 \pm 2.1$	$97.3 \pm 2.1$	-	$95.6 \pm 0.6^{*\dagger}$
	<b>10</b>	$92.9 \pm 1.7^*$	$88.7 \pm 2.6^*$	-	-
	<b>13</b>	$89.3 \pm 0.9^*$	$81.9 \pm 1.1^*$	-	$89.6 \pm 1.4^{*\dagger}$
	<b>17</b>	$84.9 \pm 1.4^{*\dagger}$	$76.8 \pm 2.3^{*\dagger}$	-	$68.9 \pm 0.6^{*\dagger}$
	<b>20</b>	-	-	-	-
	<b>Mean</b>	$88.7 \pm 1.6^*$	$86.2 \pm 2.2^*$	-	$84.7 \pm 2.8^{*\dagger}$

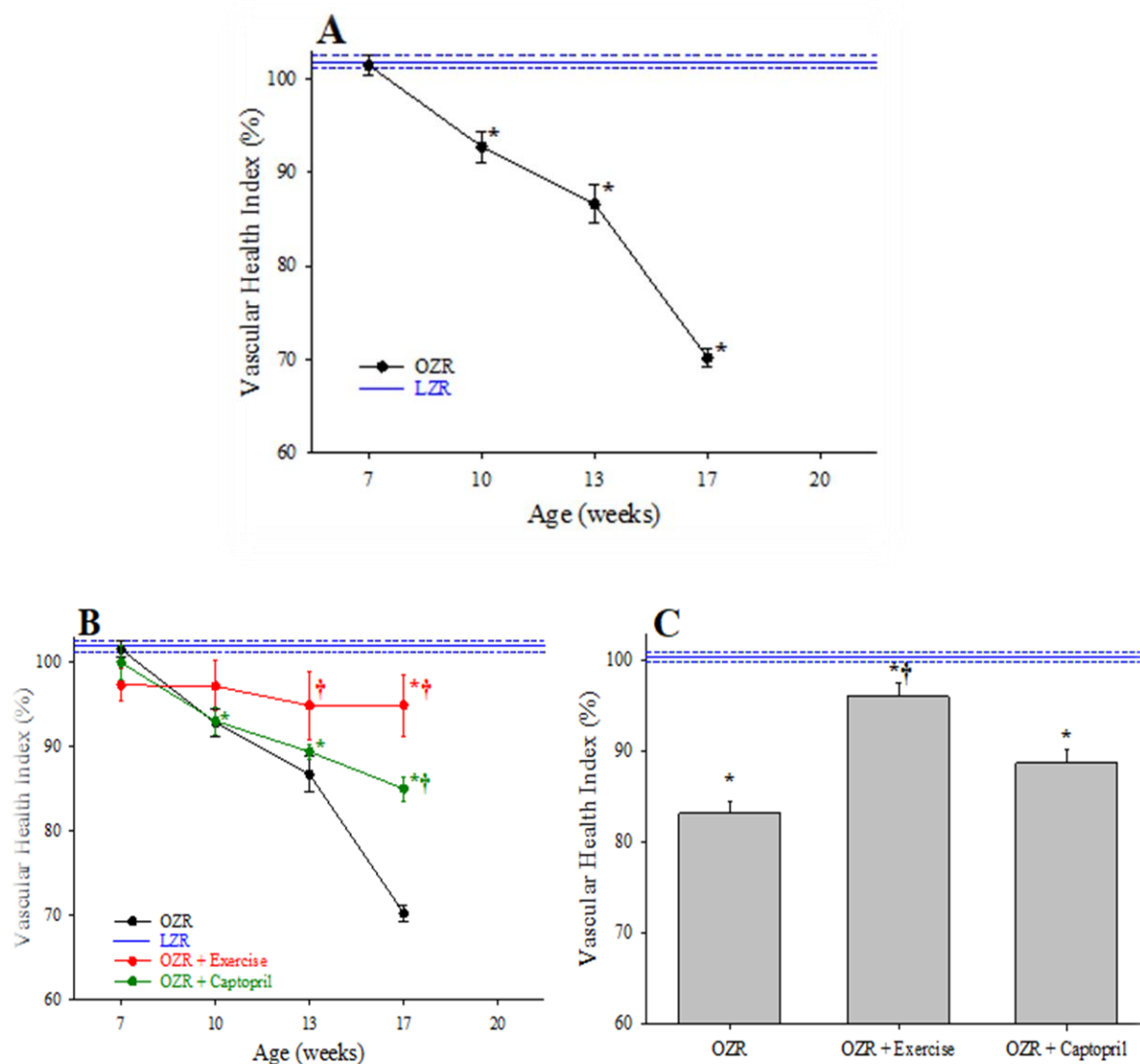


**Figure 2-2: 5 parameter peripheral (skeletal) VHI data**

Data describing the 5-parameter determination of Vascular Health Index (VHI) within the peripheral/skeletal muscle microcirculation. Data (mean $\pm$ SE) are presented for OZR over the age ranges of the present study (Panel A) or the impact of chronic interventions with either exercise or captopril administration (Panel B). Panel C presents the aggregate VHI from the different animal groups where all ages have been compiled into one data point. VHI from LZR is set to 100%, by definition. \*  $p < 0.05$  vs. LZR at that age; †  $p < 0.05$  vs. untreated OZR at that age. Please see text for details.



### *Peripheral Vascular Health Index*

Using the 5 component analyses described above, Figure 2, panel A summarizes the changes to the VHI in the peripheral microcirculation of OZR as compared to the control level of function in LZR (defined as 100%). With the progressive development of metabolic disease in OZR, there was a steady and significant decline in the magnitude of VHI throughout the age ranges used in the present study, culminating at 17 weeks of age. Figure 2, panel B presents the impact of two chronic interventions, treatment with the anti-hypertensive drug captopril and daily treadmill exercise of moderate intensity on VHI in OZR. Both interventions were effective at significantly improving skeletal muscle VHI as compared to levels determined in untreated control OZR, with chronic exercise resulting in a larger improvement to VHI as compared to that with anti-hypertensive therapy. Panel C presents the aggregate VHI score (i.e., all ages collapsed into one measurement of VHI) for OZR under control conditions and with chronic exercise and captopril interventions. While the aggregate VHI in OZR was significantly reduced as compared to LZR, the interventions with chronic exercise or captopril treatment resulted in significant improvements to aggregate VHI.

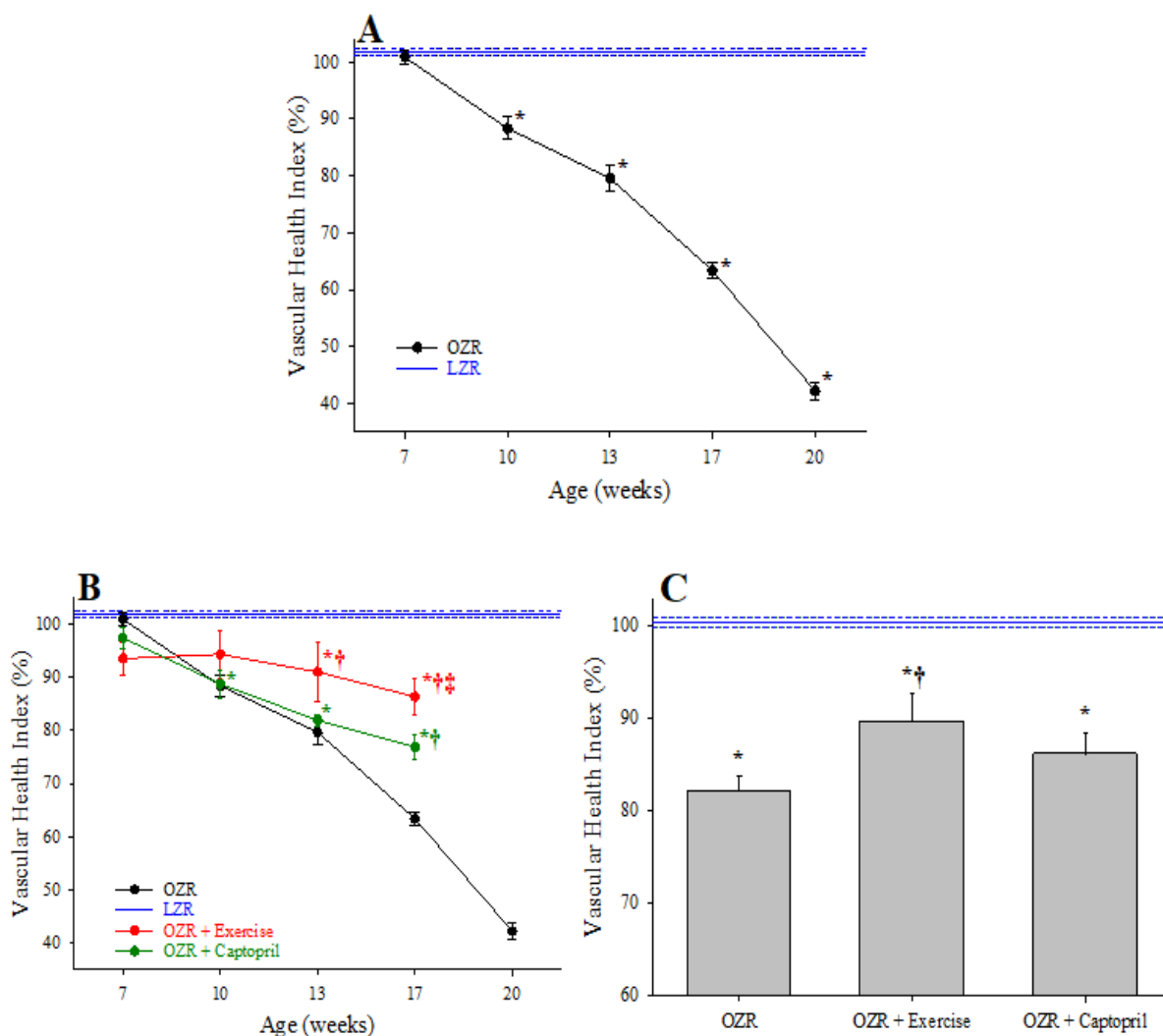


**Figure 2-3: 3 parameter VHI of peripheral (skeletal muscle) microcirculation**

Data describing the 3-parameter determination of Vascular Health Index (VHI) within the peripheral/skeletal muscle microcirculation. Data (mean±SE) are presented for OZR over the age ranges of the present study (Panel A) or the impact of chronic interventions with either exercise or captopril administration (Panel B). Panel C presents the aggregate VHI from the different animal groups where all ages have been compiled into one data point. VHI from LZR is set to 100%, by definition. \*  $p < 0.05$  vs. LZR at that age; †  $p < 0.05$  vs. untreated OZR at that age. ‡  $p < 0.05$  vs. OZR+captopril at that age. Please see text for details.

Figure 3, panel A presents the results of the 3-component analyses on skeletal muscle VHI in OZR with increasing age. While a similar trend was determined in terms of the decay in VHI in control OZR with the development of metabolic disease versus LZR as compared to that for the 5 component analyses, the calculated severity of the impairment was greater, reaching 40% of control LZR levels by 20 weeks of age. As presented in Panel B, chronic treatment with either captopril or treadmill exercise significantly improved VHI outcomes in OZR as compared to the untreated condition, with exercise being significantly more effective than captopril treatment. As presented in Panel C, chronic intervention with exercise improved VHI from levels determined in untreated OZR, although this effect was not significant with captopril treatment alone.

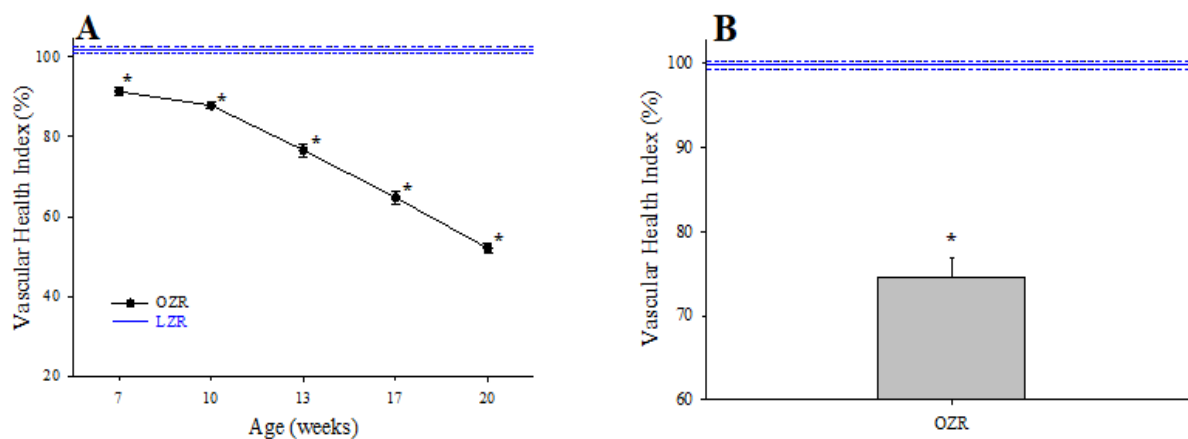


**Figure 2-4: 5 parameter VHI of cerebral circulation**

*Data describing the 5-parameter determination of Vascular Health Index (VHI) within the cerebral microcirculation. Data (mean $\pm$ SE) are presented for OZR over the age ranges of the present study (Panel A). Panel B presents the aggregate VHI from OZR where all ages have been compiled into one data point. VHI from LZR is set to 100%, by definition. \*  $p < 0.05$  vs. LZR at that age. Please see text for details.*

**Cerebral Vascular Health Index:** Using the 5-component calculation for VHI, the changes in cerebral microvascular health in OZR are presented in Figure 4. As compared to responses in control LZR, there was a progressive and significant reduction in cerebral VHI in OZR throughout the age range of the present study, reaching a maximum impairment of ~50% from that determined in LZR. It is noted that a significant impairment to cerebral VHI in OZR was already present at the earliest age range (7 weeks), where VHI was already reduced by ~10%, despite the severity of the evolving metabolic disease still being relatively mild (Table 3). The aggregate VHI for OZR across all ages is presented in Panel B, where it was significantly reduced from that calculated in untreated LZR.

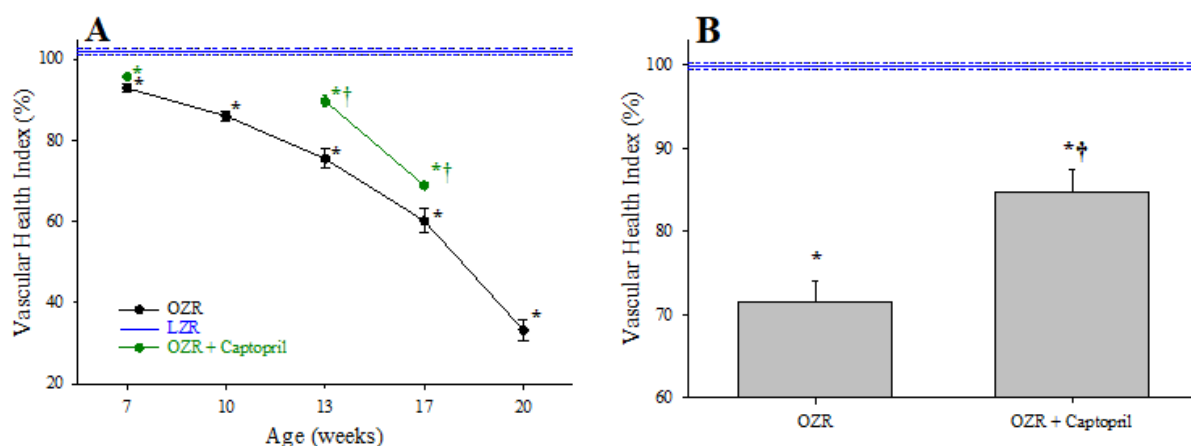


**Figure 2-5: 3 parameter VHI for cerebral microcirculation**

*Data describing the 3-parameter determination of Vascular Health Index (VHI) within the cerebral microcirculation. Data (mean±SE) are presented for OZR over the age ranges of the present study with and without chronic intervention with captopril administration (Panel A). Panel B presents the aggregate VHI from OZR, with and without captopril administration, where all ages have been compiled into one data point. VHI from LZR is set to 100%, by definition. \*  $p < 0.05$  vs. LZR at that age; †  $p < 0.05$  vs. untreated OZR at that age. Please see text for details.*

Figure 5 presents the changes to cerebral VHI using the 3-component analyses in OZR as compared to untreated LZR. The severity of the calculated impairment to cerebrovascular health was greater in OZR using the 3-parameter approach vs. the 5-component calculation, reaching only 30% of control VHI in LZR by 20 weeks of age. Also presented in Figure 5 are the results of chronic intervention with captopril on cerebral VHI, which resulted in a significant improvement to VHI as compared to that in untreated OZR at both 13 and 17 weeks of age. Panel B presents the data describing the aggregate cerebral VHI for OZR under control conditions and in response to chronic intervention with captopril. While VHI in untreated OZR was significantly reduced as compared to that in untreated LZR, chronic captopril treatment significantly improved VHI in OZR.

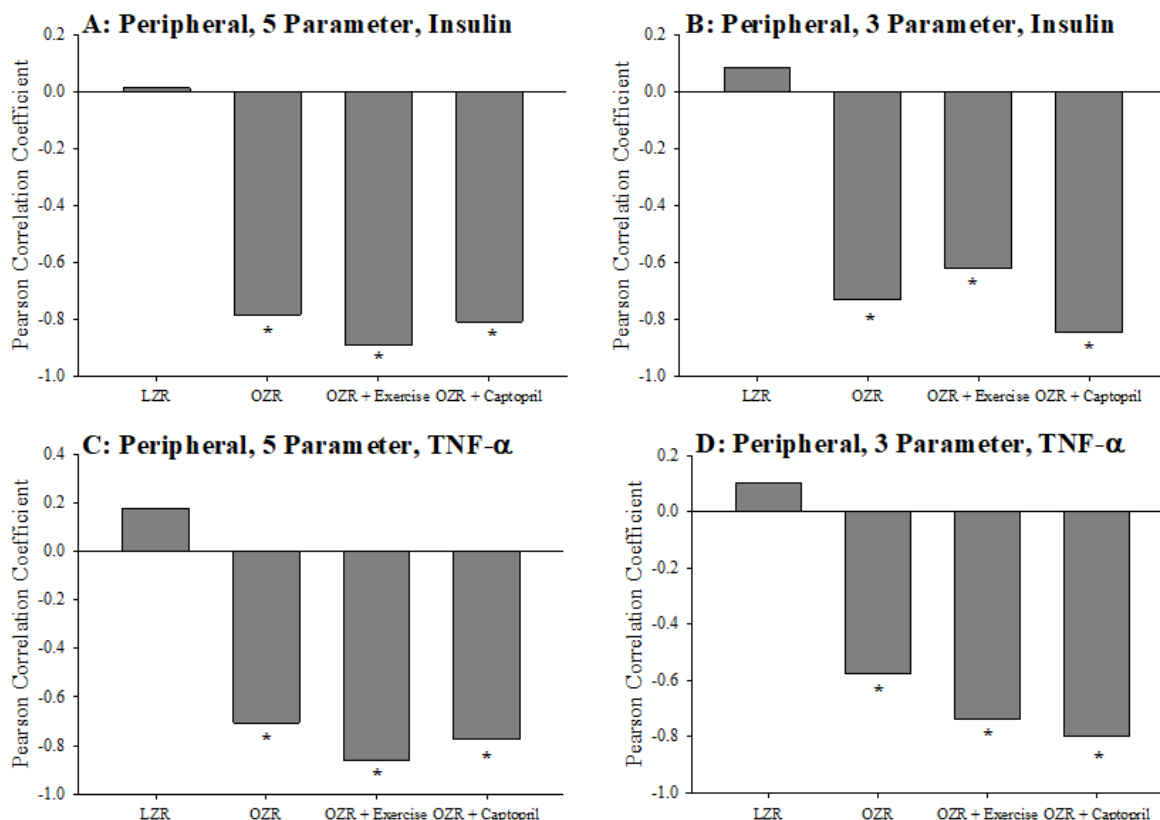


**Figure 2-6: TNF- $\alpha$  and Plasma Insulin correlations with peripheral VHI**

*Data describing the criterion validity between plasma insulin or TNF- $\alpha$  and the skeletal muscle Vascular Health Index (VHI) in the present study. The Pearson Correlation Coefficient between insulin and VHI in LZR and OZR are summarized in Panels A (5-parameter VHI) and B (3-parameter VHI). Panels C (5-parameter VHI) and D (3-parameter VHI) present the Pearson Correlation Coefficient between plasma TNF- $\alpha$  and skeletal muscle VHI in LZR and OZR. Also presented are the correlations between plasma insulin or TNF- $\alpha$  and VHI in OZR following intervention with chronic exercise or captopril treatment. \*  $p < 0.05$  vs. LZR at that age; †  $p < 0.05$  vs. OZR at that age. Please see text for details.*

### **Criterion Validity**

Figure 6 presents the criterion validity for the calculations of the peripheral VHI in the present study. In the case of the 5-component (Panel A) and the 3-component (Panel B) VHI, the plasma insulin concentration from the OZR groups were consistently and significantly negatively correlated with the vascular health index. This correlation reflects the strong tendency for OZR with a higher VHI to have the lowest insulin resistance. This similar pattern is also demonstrated for the 5-component (Panel C) and 3-component (Panel D) for the correlation between plasma  $\text{TNF-}\alpha$  and VHI in OZR where higher levels of VHI were correlated with low levels of chronic inflammation in these animals.

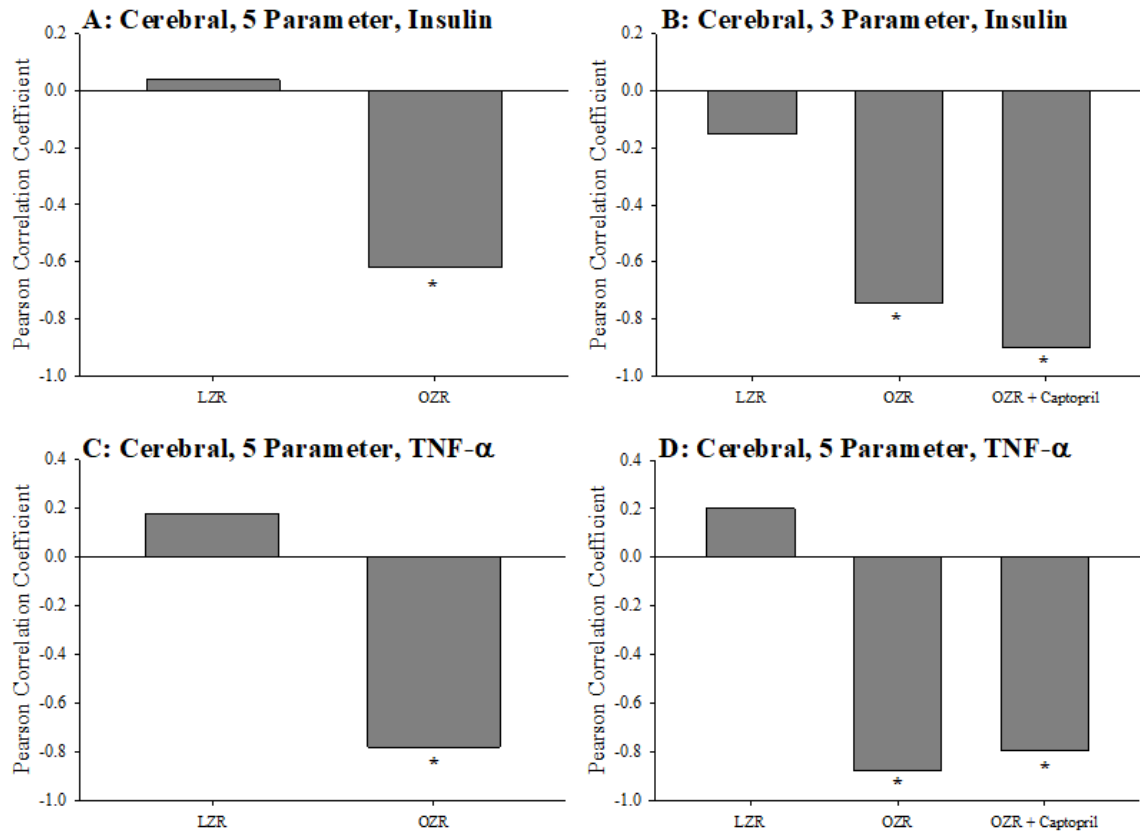


**Figure 2-7:  $\text{TNF-}\alpha$  and Plasma Insulin Correlations with Cerebral VHI**

*Data describing the criterion validity between plasma insulin or TNF- $\alpha$  and the cerebral Vascular Health Index (VHI) in the present study. The Pearson Correlation Coefficient between insulin and VHI in LZR and OZR are summarized in Panels A (5-parameter VHI) and B (3-parameter VHI). Panels C (5-parameter VHI) and D (3-parameter VHI) present the Pearson Correlation Coefficient between plasma TNF- $\alpha$  and cerebral VHI in LZR and OZR. Also presented are the correlations between plasma insulin or TNF- $\alpha$  and VHI in OZR following intervention with chronic captopril treatment. \*  $p < 0.05$  vs. LZR at that age; †  $p < 0.05$  vs. OZR at that age. Please see text for details.*

The criterion validity for the cerebral VHI calculations is summarized in Figure 7, where Panels A and B present the 5- and 3-component correlations with plasma insulin concentration, respectively. In both cases, the Pearson correlation coefficient was strongly negatively associated with VHI in OZR under untreated conditions and following chronic treatment with captopril. This same relationship was also evident for the relation between 5- (Panel C) and 3-parameter (Panel D) calculations of VHI and chronic inflammation, where the index was strongly and negatively correlated with TNF- $\alpha$ .

## 2.4 Discussion

The overall purpose for the present study was to describe an approach for developing a comprehensive metric of integrated vascular/microvascular function that is not only a valid representation of vascular health, but that also allows for the pooling of data across multiple studies to gain greater inferential power. Subsequently, we calculated this metric using our original raw data in both the skeletal muscle (peripheral) and cerebral vasculature using a 3- and 5-component version of the VHI. Finally, we demonstrated the face, content, criterion and discriminant validity of the VHI. The primary result of this



study is a validated score of integrated vascular function that can be used for more complex analytic and mechanistic modeling.

An initial question to be addressed is the utility of the VHI as it relates to an understanding of vasculopathy. When one considers a novel metric for assessing an integrated biological system, it is important to understand how the metric contributes beyond that of the individual parameters contributing to its calculation. Within the context of the present study, this is reflected as determining the superiority of VHI over individual analysis and interpretation of vascular reactivity, vascular wall mechanics and microvessel density on an individual basis. While it is certainly clear that individual metrics can provide a high-resolution inference into specific questions or hypotheses, they may be more limited in terms of understanding how complex, integrated outcomes are manifest [21], thus requiring the development of a more holistic measurement. Further, the question of “is one approach better than the other?”, may not be appropriate. In reality, multiple measures should be acting as complementary approaches where the whole may be greater than the sum of the parts. As a clinical example, while individual measurements such as obesity, smoking and blood pressure can be used to better understand a person’s cardiovascular disease risk status, the Framingham Risk Score provides a context that cannot be provided by the individual parameters it is comprised of in isolation. A comparable situation exists in the current study with the individual markers of vasculopathy and the VHI, merely for basic science research.

It is also important to note that for the development of VHI, we have included no parameter weighting, which is frequently used with other integrated metrics (such as Framingham). This lack of parameter weighting reflects two issues. First, there is no clear

*a priori* rationale for introducing parameter weighting at this time. Specifically, there is no clear evidence of the relative importance of vascular reactivity, wall mechanics or microvessel density in terms of contributions to health outcomes. While there is broad agreement that all are important and contribute, there is no consensus as to their rank ordering of importance. Second, to introduce parameter weighting at this time would reflect the use of a regression-based approach that was designed to predict an outcome. That is not the purpose of the VHI in this context (it makes no outcome predictions) and, as such, a regression-based approach was rejected in favor of the analytical approach described above.

An encompassing issue that should be considered is the selection of the different parameters that contribute to the VHI [22]. In the present study, and as presented in Figure 1, we elected to split our analyses for either skeletal muscle or cerebral VHI into both 5- and 3-parameter calculations. At the initial assessment, it was decided that indicators of endothelium-dependent and independent dilation will be important as markers of vascular reactivity. These were encompassed through acetylcholine- and hypoxia-induced dilation for endothelium-dependency in both tissues and sodium nitroprusside-induced dilation for endothelium-independency. The use of acetylcholine and/or hypoxia as a dilator stimulus also allows for a discrimination between dilator responses that are largely dependent on vascular nitric oxide bioavailability (for acetylcholine) or arachidonic acid metabolism (for hypoxia), respectively. The use of sodium nitroprusside, by contrast, allows for an estimation of vascular smooth muscle responsiveness to exogenous nitric oxide stimulation. These indices were also included as they represent some of the most commonly collected estimators of changes to vascular reactivity under conditions of altered

cardiovascular disease risk profiles and may allow for maximum utility in this regard in terms of comparisons to existing data or data between research laboratories/groups.

The presentation of VHI in the present study does not include indices of vasoconstrictor responses (e.g., phenylephrine, endothelin-1). This decision was made after extensive consideration and reflects the variability in the literature and outcomes associated with different models of disease risk. While there is evidence that vasoconstrictor responses to an exogenous challenge can be impacted by chronic disease risk conditions [23; 24], it is far from a consensus opinion and can be extremely model-dependent, especially when compared to the monumental amount of previous evidence demonstrating the impairment to dilator reactivity in both the cerebral and skeletal muscle circulations that are well correlated with outcome risk severity [23; 25; 26].

While the above metrics address alterations in vascular reactivity with changes in the risk severity, the mechanics of the vascular wall, particularly the progressive loss of wall distensibility, is considered one of the key changes to vascular structure and function associated with a poor health outcome. To that end, the slope ( $\beta$ ) of the circumferential wall stress versus strain relationship was included as an optimal parameter for the calculations of VHI [22]. This parameter has been very well correlated with the cardiovascular and cerebrovascular disease risk severity for many years [27; 28; 29] and is a critical component to the determination of VHI. Through its inclusion, we now can account for the increase in vessel stiffness with elevated risk (or following imposed interventions) and we have a critical marker of vascular mechanics at the individual vessel level of resolution.

The final parameter that was included in the calculations of VHI was that of skeletal muscle or cerebral cortex microvessel density (MVD). From a purely conceptual perspective, this adds insight and information from the “vascular network” level of resolution and speaks directly to the importance of vascularity/capillarity within the tissue under the spectrum of experimental conditions. The existing literature is replete with examples of how MVD, determined using multiple methodologies, changes with elevated disease risk and following therapeutic interventions [30; 31; 32]. The ability to include data and insight into both the pro-angiogenic and rarefactory stimuli under an array of experimental conditions is critical for assessing the overall health and functional outcomes of the tissue. Further, it also provides direct evidence for the integrated processes of mass transport and exchange at the level of the blood-tissue exchange (BTEX) unit in both skeletal muscle and the brain [33; 34]. Providing insight at this more encompassing level of spatial resolution is a central aspect of the VHI and improves its utility significantly beyond that of data pertaining to individual vessel function alone.

Taken together, the indices included in the VHI metric provide for multiple measures of vascular reactivity, and measures of vascular wall mechanics and microvascular network structure. While the 5-parameter VHI incorporates all these measures, the 3-parameter measure has the benefit of being simpler to use, with somewhat easier data collection requirements, and retains the multi-scale benefit of the 5-parameter calculation. In addition, the outcomes from both the 3- and 5-parameter calculation are extremely consistent and compare very favorably to each other in terms of interpreting vascular health/dysfunction severity. From the perspective of criterion validity, plasma biomarkers that have been well-established markers of chronic metabolic disease severity,

plasma insulin (Figure 6) and TNF- $\alpha$  (Figure 7) concentrations, demonstrated a strong negative correlation with VHI in OZR under untreated control conditions and reflected appropriate changes as a result of the imposed interventions. Minimal correlation was demonstrated with VHI in healthy LZR.

Vascular dysfunction associated with the progression of metabolic disease and other conditions of elevated cardiovascular disease risk represents a diverse group of impairments to vascular tone, wall mechanics, and network geometry. The use of a singular integrated measure that can capture these impairments while accounting for age and allowing for the pooling of data is crucial in the pursuit of more focused, innovative approaches to studying vascular dysfunction in the animal models. In the results of the present study, the VHI clearly indicates that the decline in integrated microvascular structure and function with the progression of metabolic disease in male OZR was significant, multi-factorial, and was consistent over multiple years, multiple cohorts of animals, and – perhaps most importantly – over multiple groups of investigators collecting the data/results. While the contributing mechanisms for the shift in vascular reactivity [25; 26], vascular wall mechanics [27; 28] and microvessel density [30; 31] have been extensively presented and discussed elsewhere, this speaks directly to the discriminant validity of the VHI metric and is also evident in Panels C of Figures 2 and 3 and Panels B in Figures 3 and 4.

As summarized in Table 6, regardless of 3- or 5-parameter calculation, in the skeletal muscle or cerebral vasculature, the resulting VHI presented clear and reproducible statistical differences between LZR and OZR. These results were not only present at the appropriate ages, depending on disease severity, they were also present to the appropriate

extent at the different ages (i.e., differences at 10 weeks of age were not as pronounced as differences at 17 weeks of age). Further, intervention with chronic treatment with captopril, an anti-hypertensive agent that works through inhibition of angiotensin converting enzyme resulted in a significant, appropriately delayed, improvement to VHI that reflected previously demonstrated improvements to reactivity [7; 35], wall mechanics and MVD.

***Applications of the metric:*** One of the most fundamental aspects of introducing a new metric for assessing the status of a physiological system function is determining how it can be applied most meaningfully. The development of the VHI, both the 3- and 5-parameter calculations, allows for a simple and accurate determination of the relative vascular health profile in an animal model as well as the determination of statistically significant differences in integrated vascular health outcomes between animal cohorts undergoing different interventions. In addition, the use of VHI allows for linking of datasets across time, experiments and research groups/investigators which can make comparisons of outcomes both more manageable and accessible. While VHI, taken in conjunction with other established disease risk scores and relevant biomarkers, can be used to analyze relationships between vascular health and the development of chronic pathological states, sexual dimorphism, chronic interventions, etc., it also has the ability to identify potential subgroups within analyzed datasets. Ultimately, this may have the potential to better understand disease etiology and development from the perspective of vascular dysfunction.

A version of this chapter has been published: Menon NJ, Halvorson BD, Alimorad GH, Frisbee JC, Lizotte DJ, Ward AD, Goldman D, Chantler PD, Frisbee SJ. A novel vascular health index: Using data analytics and population health to facilitate mechanistic modeling of microvascular status. *Front Physiol.* 2022 Dec 6;13:1071813. doi: 10.3389/fphys.2022.1071813. PMID: 36561210; PMCID: PMC9763931.

## 2.5 Literature Cited

- [1] M. Koenen, M.A. Hill, P. Cohen, and J.R. Sowers, Obesity, Adipose Tissue and Vascular Dysfunction. *Circ Res* 128 (2021) 951-968.
- [2] J.D. Imig, Eicosanoid blood vessel regulation in physiological and pathological states. *Clin Sci (Lond)* 134 (2020) 2707-2727.
- [3] Y. Zhou, H. Li, and N. Xia, The Interplay Between Adipose Tissue and Vasculature: Role of Oxidative Stress in Obesity. *Front Cardiovasc Med* 8 (2021) 650214.
- [4] A. Daniele, S.J.E. Lucas, and C. Rendeiro, Detrimental effects of physical inactivity on peripheral and brain vasculature in humans: Insights into mechanisms, long-term health consequences and protective strategies. *Front Physiol* 13 (2022) 998380.
- [5] D.K. Sandsmark, A. Bashir, C.L. Wellington, and R. Diaz-Arrastia, Cerebral Microvascular Injury: A Potentially Treatable Endophenotype of Traumatic Brain Injury-Induced Neurodegeneration. *Neuron* 103 (2019) 367-379.
- [6] K.A. Lemaster, S.J. Frisbee, L. Dubois, N. Tzemos, F. Wu, M.T. Lewis, R.W. Wiseman, and J.C. Frisbee, Chronic atorvastatin and exercise can partially reverse established skeletal muscle microvasculopathy in metabolic syndrome. *Am J Physiol Heart Circ Physiol* 315 (2018) H855-H870.
- [7] S.J. Frisbee, S.S. Singh, D.N. Jackson, K.A. Lemaster, S.A. Milde, J.K. Shoemaker, and J.C. Frisbee, Beneficial Pleiotropic Antidepressive Effects of Cardiovascular Disease Risk Factor Interventions in the Metabolic Syndrome. *J Am Heart Assoc* 7 (2018).
- [8] K.T. Fredricks, Y. Liu, and J.H. Lombard, Response of extraparenchymal resistance arteries of rat skeletal muscle to reduced PO<sub>2</sub>. *Am J Physiol* 267 (1994) H706-15.
- [9] Y. Liu, K.T. Fredricks, R.J. Roman, and J.H. Lombard, Response of resistance arteries to reduced PO<sub>2</sub> and vasodilators during hypertension and elevated salt intake. *Am J Physiol* 273 (1997) H869-77.
- [10] K.T. Fredricks, Y. Liu, N.J. Rusch, and J.H. Lombard, Role of endothelium and arterial K<sup>+</sup> channels in mediating hypoxic dilation of middle cerebral arteries. *Am J Physiol* 267 (1994) H580-6.



- [11] G.L. Baumbach, and M.A. Hajdu, Mechanics and composition of cerebral arterioles in renal and spontaneously hypertensive rats. *Hypertension* 21 (1993) 816-26.
- [12] S.D. Brooks, S.M. Hileman, P.D. Chantler, S.A. Milde, K.A. Lemaster, S.J. Frisbee, J.K. Shoemaker, D.N. Jackson, and J.C. Frisbee, Protection from vascular dysfunction in female rats with chronic stress and depressive symptoms. *Am J Physiol Heart Circ Physiol* 314 (2018) H1070-H1084.
- [13] W.R. Milnor, *Hemodynamics*, Williams & Wilkins, Baltimore, 1982.
- [14] F. Hansen-Smith, A.S. Greene, A.W. Cowley, Jr., and J.H. Lombard, Structural changes during microvascular rarefaction in chronic hypertension. *Hypertension* 15 (1990) 922-8.
- [15] A.S. Greene, J.H. Lombard, A.W. Cowley, Jr., and F.M. Hansen-Smith, Microvessel changes in hypertension measured by Griffonia simplicifolia I lectin. *Hypertension* 15 (1990) 779-83.
- [16] J.C. Frisbee, A.G. Goodwill, S.J. Frisbee, J.T. Butcher, R.W. Brock, I.M. Olfert, E.R. DeVallance, and P.D. Chantler, Distinct temporal phases of microvascular rarefaction in skeletal muscle of obese Zucker rats. *Am J Physiol Heart Circ Physiol* 307 (2014) H1714-28.
- [17] J.C. Frisbee, Remodeling of the skeletal muscle microcirculation increases resistance to perfusion in obese Zucker rats. *Am J Physiol Heart Circ Physiol* 285 (2003) H104-11.
- [18] D.H. Munzenmaier, and A.S. Greene, Chronic angiotensin II AT1 receptor blockade increases cerebral cortical microvessel density. *Am J Physiol Heart Circ Physiol* 290 (2006) H512-6.
- [19] P.D. Chantler, C.D. Shrader, L.E. Tabone, A.C. d'Audiffret, K. Huseynova, S.D. Brooks, K.W. Branyan, K.A. Grogg, and J.C. Frisbee, Cerebral Cortical Microvascular Rarefaction in Metabolic Syndrome is Dependent on Insulin Resistance and Loss of Nitric Oxide Bioavailability. *Microcirculation* 22 (2015) 435-45.
- [20] P. Price, Jhangiani, R., & Chiang, I., *Research Methods of Psychology*, BCcampus, Victoria, BC, 2015.

- [21] K. Lemaster, D. Jackson, D. Goldman, and J.C. Frisbee, Insidious incrementalism: The silent failure of the microcirculation with increasing peripheral vascular disease risk. *Microcirculation* 24 (2017).
- [22] R.M. Effros, H. Schmid-Schönbein, and J. Ditzel, *Microcirculation, current physiologic, medical, and surgical concepts*, Academic Press, New York, 1981.
- [23] P.A. Stapleton, M.E. James, A.G. Goodwill, and J.C. Frisbee, Obesity and vascular dysfunction. *Pathophysiology* 15 (2008) 79-89.
- [24] K. Lemaster, D. Jackson, D.G. Welsh, S.D. Brooks, P.D. Chantler, and J.C. Frisbee, Altered distribution of adrenergic constrictor responses contributes to skeletal muscle perfusion abnormalities in metabolic syndrome. *Microcirculation* 24 (2017).
- [25] J. Zhang, Biomarkers of endothelial activation and dysfunction in cardiovascular diseases. *Rev Cardiovasc Med* 23 (2022) 73.
- [26] G. Benincasa, E. Coscioni, and C. Napoli, Cardiovascular risk factors and molecular routes underlying endothelial dysfunction: Novel opportunities for primary prevention. *Biochem Pharmacol* 202 (2022) 115108.
- [27] S. Laurent, C. Agabiti-Rosei, R.M. Bruno, and D. Rizzoni, Microcirculation and Macrocirculation in Hypertension: A Dangerous Cross-Link? *Hypertension* 79 (2022) 479-490.
- [28] P. Lacolley, V. Regnault, and S. Laurent, Mechanisms of Arterial Stiffening: From Mechanotransduction to Epigenetics. *Arterioscler Thromb Vasc Biol* 40 (2020) 1055-1062.
- [29] S. Laurent, J. Cockcroft, L. Van Bortel, P. Boutouyrie, C. Giannattasio, D. Hayoz, B. Pannier, C. Vlachopoulos, I. Wilkinson, H. Struijker-Boudier, and A. European Network for Non-invasive Investigation of Large, Expert consensus document on arterial stiffness: methodological issues and clinical applications. *Eur Heart J* 27 (2006) 2588-605.
- [30] A. Wong, S.Q. Chen, B.D. Halvorson, and J.C. Frisbee, Microvessel Density: Integrating Sex-Based Differences and Elevated Cardiovascular Risks in Metabolic Syndrome. *J Vasc Res* 59 (2022) 1-15.

- [31] S. Paavonsalo, S. Hariharan, M.H. Lackman, and S. Karaman, Capillary Rarefaction in Obesity and Metabolic Diseases-Organ-Specificity and Possible Mechanisms, Cells, NLM (Medline), 2020.
- [32] J. Liang, Y. Li, L. Chen, W. Xia, G. Wu, X. Tong, C. Su, J. He, X. Lin, and J. Tao, Systemic microvascular rarefaction is correlated with dysfunction of late endothelial progenitor cells in mild hypertension: a substudy of EXCAVATION-CHN1. *J Transl Med* 17 (2019) 368.
- [33] P.M. McClatchey, J.C. Frisbee, and J.E.B. Reusch, A conceptual framework for predicting and addressing the consequences of disease-related microvascular dysfunction. *Microcirculation* 24 (2017).
- [34] P. Mason McClatchey, F. Wu, I.M. Olfert, C.G. Ellis, D. Goldman, J.E.B. Reusch, and J.C. Frisbee, Impaired Tissue Oxygenation in Metabolic Syndrome Requires Increased Microvascular Perfusion Heterogeneity. *J Cardiovasc Transl Res* 10 (2017) 69-81.
- [35] J.C. Frisbee, Hypertension-independent microvascular rarefaction in the obese Zucker rat model of the metabolic syndrome. *Microcirculation* 12 (2005) 383-92.

## Chapter 3

### Bridge Section

The development of an integrated vascular health index is an important area of research that has the potential to improve our understanding of microvascular status and its impact on disease etiology, progression and treatment. In the second chapter of this thesis, the development of a novel vascular health index was outlined and validated using data analytics of direct vascular measures in lean Zucker rats and their obese counterparts to ultimately yield an integrated measure of vascular health. While the second chapter utilized our novel VHI to explore the ameliorating effect of exercise and an angiotensin converting enzyme inhibitor (captopril), on the microvascular health status of obese Zucker rats, the next question to be addressed was the use of this novel index to study the effects of many established pharmacological interventions in a pre-clinical model of metabolic disease.

The novel vascular health index developed in the second chapter of this thesis presented an integrated measure of vascular health that simultaneously accounts for vascular reactivity, wall mechanics and network geometry to provide a more comprehensive picture of microvascular status. This index facilitates the use of data analytics and population health to improve our understanding of vascular health. By collecting and analyzing large amounts of data, we can identify patterns and trends that are not visible using traditional methods. This can then be used to develop more accurate models of microvascular status. In this way, the novel vascular health index can help facilitate mechanistic modeling of microvascular status, providing a more complete picture of the health of the vascular system.

The methodology used to create the index and the key results obtained from this analysis were discussed in detail. The potential significance of these findings for the field of vascular health was also explored, including how the use of this novel index allows for data pooling across experiments, time and research groups thereby expanding the sources of data available to basic scientists to fill a gap in the current understanding of

microvascular status and how this could lead to better detection and management of vascular dysfunction in the future.

The next logical step in the development and application of the VHI was to determine the impact of pharmacological intervention on microvascular health, using the novel index as a tool for evaluation. This was a natural next step, given the potential benefits of the novel index identified in the first paper. The findings in the second paper provided valuable insights into the effectiveness of specific pharmacological interventions in managing symptoms of metabolic disease and preserving microvascular health.

Therefore, the development of the novel vascular health index in the first paper was crucial in guiding our investigation into the impact of pharmacological intervention on microvascular health in the second paper. The findings from both papers have contributed to a deeper understanding of microvascular health and its relationship with metabolic disease and have helped to pave the way for further research in this area.

### **3 Integrated article 2: Application of a novel index for understanding vascular health following pharmacological intervention in a pre-clinical model of metabolic disease**

#### **3.1 Introduction**

The role and relevance of microvascular dysfunction as a significant contributor to the functional or clinical outcomes under the broader umbrella of cardio- or cerebrovascular disease risk has long been an area of great focus in both basic and translational research. However, although many diverse efforts have been made to investigate individual correlative measures and predictive biomarkers of vascular dysfunction, far fewer have attempted to understand and frame integrated vascular function within the context of health, disease, and treatment. [1; 2]

We identify three key challenges that impede a more integrated analysis of vascular function. First, despite expanded insight into the emergence and impact of metabolic diseases on health outcomes, the interpretation of data can be complicated as a result of the multi-variate nature of not only microvascular structure and function, but the temporal development of these adaptations to disease risk. Second, although they are powerful in terms of understanding the diversity of disease and in facilitating investigations evaluating the broader relative dysfunctional states of the vasculature in various disease states and pharmacological treatment regimes, heterogeneity and diversity in models of vasculopathy that are used further complicate efforts to integrate datasets and thereby to produce opportunities for more detailed, powerful advanced analytic approaches. Third, basic science investigators face challenges when integrating results across multiple laboratories because differences in goals, methodology and expertise may not allow facile merging of datasets.

Given that the overwhelming majority of individual research efforts have a complex study design with highly specialized protocols/preparations chosen to support or refute a specific hypothesis or question, it can be problematic to use resulting data beyond the initial intent of each study. This hinders our ability to create integrated secondary data sources from which results can be pooled for greater analytic and inferential power, and profoundly limits our ability to access a variety of advanced analytic approaches including machine learning, artificial intelligence and metaanalyses. In order to access such advanced techniques, basic scientists must have approaches that allow for the pooling of datasets across multiple primary studies across levels of spatial and temporal resolution that facilitate data interpretation from a broader construct of “health” and “disease”.

In response to these myriad challenges, we develop and describe a standardized, integrated measure of vascular health and dysfunction. [3] The Vascular Health Index (VHI) allows for the simultaneous assessment of changes to vascular reactivity/endothelial function, vascular wall mechanics, and microvessel density within skeletal muscle and cerebral vascular networks with the progression of chronic metabolic disease. This VHI will quantify vascular dysfunction in states of elevated peripheral vascular disease and cerebrovascular disease risk relative to the vascular function of healthy, age-matched control animals. [3] Further, the present study also focuses on the impact of clinically relevant pharmacological interventions to change VHI from untreated control conditions and can provide some insight as to why some interventions have more effective functional outcomes despite comparable impacts on specific risk factors. The impact of these pharmacologic interventions on the integrated vascular function of a network are of great interest in both the development and evaluation of prodromic and postdromic intervention targeting to achieve ideal health outcomes.

## 3.2 Materials and Methods

The majority of the data presented here have been published previously and these citations will be made at the appropriate and relevant points within the text. The present manuscript also represents the inclusion of *de novo* experiments/analyses, previously unpublished results/analyses, and the integration of data from previous studies for novel analyses. The protocols and specific methodology for the collection of the specific vascular phenotypes and the subsequent calculation of the Vascular Health Index (VHI) are detailed and referenced below.

### 3.2.1 Animal Model

All experiments and analyses described in this manuscript use male lean (LZR) and obese (OZR) Zucker rats. Animals were purchased from the supplier (Harlan/Envigo) at 6-7 weeks of age and were housed in an accredited animal care facility at the Medical College of Wisconsin, West Virginia University, or the University of Western Ontario, with *ad libitum* access to normal chow and water until the time of final usage unless otherwise noted. Following one week of acclimation, rats were placed into one of the following groups until their final usage:

4. Time control (LZR and OZR without intervention and aged to a maximum of ~20 weeks)
5. Anti-hypertensive groups:
  - a) OZR treated with captopril (angiotensin converting enzyme inhibitor;  $60 \text{ mg}\cdot\text{kg}^{-1}\cdot\text{day}^{-1}$ ; mixed with food; [4; 5])
  - b) OZR treated with hydralazine (smooth muscle hyperpolarizer/vasodilator;  $50 \text{ mg}\cdot\text{kg}^{-1}\cdot\text{day}^{-1}$ ; mixed with food; [4; 5])
6. Anti-dyslipidemia groups (skeletal muscle VHI only):
  - a) OZR treated with atorvastatin (HMG Co-A [3-hydroxy-3-methyl-glutaryl-coenzyme A reductase] reductase inhibitor);  $25 \text{ mg}\cdot\text{kg}^{-1}\cdot\text{day}^{-1}$ ; mixed with food [4; 6])
  - b) OZR treated with gemfibrozil (peroxisome proliferator-activated receptor- $\alpha$  activator);  $100 \text{ mg}\cdot\text{kg}^{-1}\cdot\text{day}^{-1}$ ; mixed with food [4; 6])
7. Anti-diabetes groups (cerebral VHI only):
  - a) OZR treated with metformin (hepatic gluconeogenesis inhibitor;  $300 \text{ mg}\cdot\text{kg}^{-1}\cdot\text{day}^{-1}$ ; drinking water [4; 7])
  - b) OZR treated with rosiglitazone (insulin sensitizing agent;  $10 \text{ mg}\cdot\text{kg}^{-1}\cdot\text{day}^{-1}$ ; mixed with food; [4; 7])



8. Antioxidant/Anti-inflammatory/Nitric oxide bioavailability groups:
  - a) OZR treated with TEMPOL (antioxidant);  $10^{-3}$  mol/L  $\bullet$ day $^{-1}$ ; mixed in drinking water [4; 8])
  - b) OZR treated with pentoxifylline (skeletal muscle VHI only; inhibition of tumour necrosis factor alpha (TNF- $\alpha$ ) production; 30 mg $\bullet$ kg $^{-1}$  $\bullet$ day $^{-1}$ ; i.p. injection [4])
  - c) OZR treated with L-NAME (L-N<sup>G</sup>-Nitro arginine methyl ester; non-selective nitric oxide synthase inhibitor);  $10^{-4}$ M, in drinking water [4; 9])

Throughout the treatment of rats with the agents listed above, changes in body mass as well as daily food and water consumption with age were taken into account to maintain proper dosing as well as changes to circulating blood volume [4; 6; 10].

At the time of final usage, each rat was deeply anesthetized with sodium pentobarbital (50 mg $\bullet$ kg $^{-1}$  i.p.) and the trachea was intubated to maintain a patent airway. In all rats, a carotid artery and an external jugular vein were cannulated to measure arterial pressure and to infuse additional anesthetic, respectively, as necessary. At this time, an aliquot of blood was drawn from the jugular vein of each animal to be used for the subsequent determination of plasma metabolic/endocrine, oxidant stress, and inflammatory biomarker profiles using commercially available kits [4]. All procedures followed approved IACUC protocols at each institution.

***Evaluation of Vascular Reactivity:*** The assessment of arteriolar reactivity from skeletal muscle was determined using the intramuscular continuation of the gracilis arteries, which were removed from each leg following the procedures in the neck (above). Subsequently, the rat was given a lethal overdose of pentobarbital anesthetic, followed by the removal of the head via decapitation. For the assessment of cerebrovascular reactivity, the middle

cerebral arteries (MCA) were removed from their origin on the Circle of Willis following the removal of the brain from the skull. Both the gracilis muscle arterioles and the MCAs were doubly-cannulated and placed in a heated chamber (37°C) that allowed the vessel lumen and exterior to be perfused and superfused, respectively, with physiological salt solution (PSS; equilibrated with 21% O<sub>2</sub>, 5% CO<sub>2</sub>; 74% N<sub>2</sub>) from separate reservoirs [11; 12]. Vessel diameter was measured using television microscopy and an on-screen video micrometer. Both vessels were extended to their *in situ* length and were equilibrated at 80% of the animal's mean arterial pressure [11; 13].

In both gracilis muscle arterioles and MCAs, vascular reactivity was evaluated in response to application of increasing concentrations of acetylcholine (10<sup>-9</sup> M – 10<sup>-6</sup> M) in order to assess endothelial function and dilator responses [11; 14].

The mechanical responses of isolated arterioles following pharmacological challenge with any of the agonists were fit with the following logistic equation:

$$y = \text{min} + \left[ \frac{\text{max} - \text{min}}{1 + 10^{\log EC_{50} - x}} \right]$$

where  $y$  represents the change in arteriolar diameter, “min” and “max” represent the lower and upper bounds, respectively, of the change in arteriolar diameter with increasing acetylcholine concentration,  $x$  is the logarithm of acetylcholine concentration and  $\log EC_{50}$  represents the logarithm of acetylcholine concentration ( $x$ ) at which the response ( $y$ ) is halfway between the lower and upper bounds.

***Evaluation of Vascular Wall Mechanics:*** Following the experimental procedures for

measuring *ex vivo* vascular reactivity for both MCA and gracilis arterioles, the perfusate and superfusate PSS were replaced with  $\text{Ca}^{2+}$ -free PSS containing the metal ion chelators EDTA (0.03mM) and EGTA (2.0mM). Vessels were challenged with  $10^{-7}$  M phenylephrine (gracilis arterioles) or serotonin (middle cerebral arteries) until all active tone was lost. Subsequently, intraluminal pressure within the isolated vessel was altered, in 20 mmHg increments, between 0 mmHg and 160 mmHg. To ensure that a negative intraluminal pressure was not exerted on the vessel, 5 mmHg was used as the “0 mmHg” intraluminal pressure point; all other values of intraluminal pressure were multiples of 20 mmHg up to 160 mmHg. After ~5 minutes at each intraluminal pressure, the inner and outer diameter of the isolated vessel was determined.

All calculations of arteriolar wall mechanics (used as indicators of structural alterations to the individual microvessel) are based on those used previously [15; 16]. The resulting stress versus strain relationship from each vessel was fit (ordinary least squares analyses,  $r^2 > 0.85$ ) with an exponential growth equation, where higher levels of slope ( $\beta$ ) are indicative of increasing arterial stiffness (i.e., requiring a greater degree of distending pressure to achieve a given level of wall deformation; [15; 17]).

***Evaluation of Skeletal Muscle Microvessel Density:*** From each rat, the gastrocnemius muscle from the left leg was removed, rinsed in PSS and fixed in 0.25% formalin. Muscles were embedded in paraffin and cut into 5  $\mu\text{m}$  cross sections. Sections were incubated with *Griffonia simplicifolia* I lectin (GS-1; a general microvessel stain for all vessel  $< 20 \mu\text{m}$  diameter; [18; 19], for subsequent determination of microvessel density using immunohistochemistry and fluorescence microscopy for the microvessel counting

procedures [8; 20].

***Determination of Cerebral Cortex Microvessel Density:*** Following removal of the MCAs from the Circle of Willis on the base of the brain, the brain was placed within Tissue-Tek OCT compound and frozen. Brains were then sliced into 5  $\mu\text{m}$  cross sections and were then stained using the established approach developed previously using primary anti-CD-31 antibody [7; 21]. Under microscopy, localization of labeled microvessels and subsequent microvessel counting procedures were done as described previously [7].

### 3.2.2 Determining VHI characteristics

In developing the VHI and ensuring it can effectively capture critical aspects of vascular structure and function, the following fundamental considerations were made:

- 6) Given the many structural and functional differences exist between the cerebral and skeletal muscle vasculature, a metric representing the health of their vasculature must be calibrated and calculated separately to yield a cerebral VHI and a peripheral VHI.
- 7) The metric must be a composite measure that accounts for distinct and relevant aspects of vascular function and structure.
- 8) The metric will not be a predictive measure but instead will describe the relative state of the vasculature at a given time. Given this, there is no *a priori* basis for establishing parameter weighting or coefficients for the different components within the composite metric. That is, all components of the VHI are given equal weighting.
- 9) The use and calculation of such a metric needs to be practical and feasible. As such, the components of the metric need to be relatively easily collected in sufficient frequency to facilitate the actual quantitative determination of the metric in significant amounts, not just for our research group but other interested research teams as well.
- 10) Given that the validity of a metric is the degree to which values from that metric represent the

variable they intend to, we will need several forms of evidence to establish VHI as a valid estimator of vascular health. The specific forms of evidence/aspects of validity of concern are:

- e) **Face validity [22]:** the extent to which a metric appears to measure the construct of interest; are the parameters used in the development of the metric appropriate to the intention?

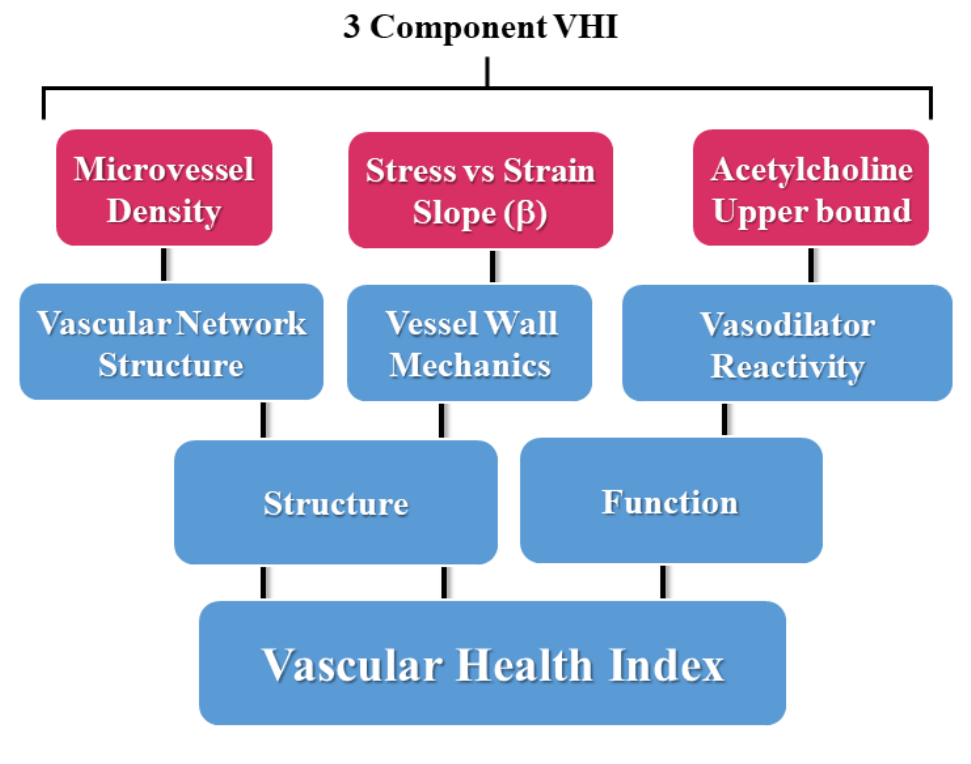


**Figure 3-1: VHI Component schematic**

*Schematic representation of the components contributing to the three-parameter calculations for the Vascular Health Index (VHI), and their context within the scope of vascular structure and function. Please see text for details.*

- f) **Content Validity [22]:** determines whether the index is appropriately representative of the aspects of the system being modeled. Does the content of the metric encompass the relevant aspects it is intended to estimate?
- g) **Criterion Validity [22]:** the extent to which the index responds in a manner that is

consistent with general understanding and developed hypotheses and represents how well the value of the metric is indicative of the underlying theory of the system. Specifically, it is the extent to which values of a metric are correlated with other criterion variables with which one would expect the measure to be correlated.

- h) **Discriminant Validity [22]:** the ability of the metric to distinguish between cohorts with differing levels of the underlying construct (in this case, vascular health). For example, VHI must be able to distinguish a cohort of OZR from LZR as well as any effective treatment group that works to mitigate or minimize vascular dysfunction (e.g., a population of OZR receiving a therapeutic pharmacological treatment).

In evaluating the above criteria, we developed a three–component calculation for of both cerebral and peripheral VHI in LZR and OZR. The use of a three–component metric (comprised of readily collected measures) allows for larger sample sizes to be assessed while still capturing the essential aspects of vascular health, allowing for a more facile, easily integrated and broadly applicable approach for investigators. [3] The inclusion of additional components to the calculation of VHI will, by definition, make the determination more complicated, requiring more extensive and diverse data collection, with the potential introduction of greater error and variability, potentially confounding interpretation. The initial development of the VHI was constructed using a different dataset from that for the present study (i.e., VHI was not specifically constructed for application to the treatment effects in the current dataset.) [3]

**VHI Parameter Selection:** Three fundamental aspects of healthy vasculature are the ability of resistance vessels to respond appropriately to vasoactive stimuli, the mechanics (i.e., the distensibility or stiffness) of the arteriolar wall, and the structure of the

microvascular network from the perspective of a microvessel/capillary density within perfused tissue [23]. Thus, to ensure face validity as well as content validity, the components of the VHI were selected to represent these differing major descriptors of vascular health.

***Assessing the Four Aspects of Validity:***

***Face Validity:*** Being the weakest and least rigorous form of validity, face validity is often assessed informally. For our purposes, the assessment was made in the process of parameter selection for the components of the measure. This is represented in Figure 1, where the conceptual design summarizes the major aspects of vascular function used in the present study, where each of the domains are represented in the calculations of VHI.

***Content Validity:*** The content validity of the measure was ensured by clearly defining and restricting the components of “vascular health” to three major aspects and appropriately representing those aspects in the VHI. The three main aspects of vascular health are the reactivity of resistance vessels, arteriolar wall mechanics, and microvessel density within the tissue [23].

***Criterion Validity:*** In assessing criterion validity, we need to identify a variable with which we would expect individual values of VHI in a given population to be correlated. For the present study, both plasma insulin and TNF- $\alpha$  concentrations were selected as the criterion with an expected correlation to VHI in a population of obese Zucker rats, given the well-established demonstration of changes in their circulating concentrations with increasing severity and duration of metabolic disease [24; 25]. To demonstrate criterion

validity, there must be a strong correlation between plasma insulin and TNF- $\alpha$  concentrations and VHI in OZR through the age range of the study.

***Discriminant Validity:*** We will demonstrate the metric's discriminant validity by distinguishing specific populations of Zucker rats using only their VHI values. Specifically, cohorts of OZR that have been treated with a blocker of nitric oxide bioavailability (L-NAME) to accelerate the degradation of the three measures of vasculopathy used in the present study [8; 26].

***Construction of the measure:*** The construction of the VHI was done using data that were distinct from that in the present study with no overlap. This is an important consideration as it removes potential bias from any attempt to produce results and interpretations specific to the current data set. In constructing and calculating VHI, the following principles were used:

1. The metric will be calculated at different age points (7, 10, 13, 17, and 20 weeks old). This allows for comparisons between lean and obese Zucker rats across all ages of the animal and the resultant composite score can be considered to be independent of the specific age.
2. With "ideal" vascular health quantified in LZR, an animal experiencing an altered condition from this (e.g., elevated disease risk, interventional treatments) can then be quantitatively compared to this ideal standard. The most direct mechanism for accomplishing this is to calculate a percentage-based score, where the measurement for the "sick" animal is expressed as a percentage (%) of the value for the age-matched healthy standard. Thus, the VHI metric is interpreted as % of ideal vascular health.



3. Within each of the three components comprising VHI, the percentage scores are converted to a percentile rank. This step is taken to normalize the differing variability or ranges of values that can be demonstrated in each of the three VHI components due to scale and the (patho) physiologic range of results. VHI is meant to weigh all components equally and was not artificially dominated by any single component. This was necessary for the components used in the present study, as alterations in dilator reactivity and microvessel density in either the skeletal muscle or cerebral circulation are invariably modest as compared to changes in the slope ( $\square$ ) coefficient describing alterations to vascular wall mechanics in OZR, which can frequently be multiples of the values determine in LZR. The use of percentile ranking prevents the changes in wall mechanics from dominating the calculation of VHI. VHI is then calculated by averaging the component score (% of ideal) across three components in the index; repeated for both the cerebral and peripheral VHI.
4. To determine the index in control LZR, calculations were performed as outlined in Table 1. It should be noted that, with both age and disease risk, some variables are expected to increase as animals become unhealthy (e.g., vascular wall stiffness) whereas others are expected to decrease (e.g., endothelial function). As shown in Table 1, this has been addressed in the calculations for the vascular wall stiffness component score by treating the relative increase above the associated standard of health value as a corresponding deficit to the component score (%).
5. The metric will be a measure of “health”, where untreated LZR that served as control animals in previous studies were used to define ideal vascular function (i.e., ideal standards for each component of VHI) at different age points. Therefore, the

VHI of a given animal will represent any unhealthy deviation from normal in its vasculature. Given the use of data across multiple studies, the VHI of any age-matched animal under an experimental condition will be calculated relative to the specific control values (i.e., untreated LZR) from the original experiment.

**Statistical Analyses:** Significant differences in baseline characteristics (Table 3), skeletal VHI components (Table 4), and cerebral VHI components (Table 5) across groups were analyzed with analysis of variance (ANOVA) or repeated measures ANOVA, as appropriate, followed by Newman-Keuls post-hoc test to determine differences between specific groups. Pearson correlation coefficients between VHI and plasma insulin or VHI and TNF- $\alpha$  were calculated and used to demonstrate the association between parameters and demonstrate criterion validity.

**Table 3-1: VHI Component calculation**

<b>Component</b>	<b>Expected Deviation from LZR with Disease Risk</b>	<b>Formula used to Calculate VHI Component</b>
Acetylcholine-induced Dilation (upper bound; $\mu\text{m}$ )	Reduced ( $\downarrow$ )	$\frac{\textit{Measurement}}{\textit{Standard of health}} \times 100$
Microvessel Density ( $\#/\text{mm}^2$ )	Reduced ( $\downarrow$ )	$\frac{\textit{Measurement}}{\textit{Standard of health}} \times 100$



<b>13</b>	24	14	6	6	-	-	-	6	6	6	6
<b>17</b>	18	12	6	6	-	-	-	6	6	6	6
<b>20</b>	19	8	-	-	-	-	-	-	-	-	-

**Table 3-3: Animal baseline characteristics**

Baseline characteristics of animals used in the present study. \* p<0.05 vs. LZR at that age; † p<0.05 vs. OZR at that age.

Variable	Group	7 wk	10 wk	13 wk	17 wk	20 wk
<b>Mass (g)</b>	<b>LZR</b>	149.7±1.5†	243.0±2.1†	307.2±2.0†	357.5±1.5†	374.3±2.6†
	<b>OZR</b>	233.9±1.8*	409.4±2.6*	512.3±3.2*	682.3±2.5*	741.8±11.0*
	<b>OZR+HYD</b>	244.0±3.9*	411.5±3.4*	510.4±9.2*	606.0±4.8*†	-
	<b>OZR+CAP</b>	239.0±2.7*	409.0±4.5*	515.3±4.6*	624.3±8.6*	-
	<b>OZR+GEM</b>	257.0±4.3*†	403.7±3.6*	514.4±4.7*	631.7±5.8*†	-
	<b>OZR+ATOR</b>	246.0±1.7*†	404.5±3.2*	493.5±10.0*†	615.2±5.4*†	-
	<b>OZR+MET</b>	237.0±1.0*	-	485.0±6.1*†	658.8±4.2*†	-
	<b>OZR+ROSI</b>	246.8±2.9*	-	475.7±3.1*†	680.2±5.1*	-
	<b>OZR+TEM</b>	233.0±3.6*	412.0±11.0*	525.5±9.2*	612.0±12.7*†	-
	<b>OZR+LNM</b>	238.5±5.1*	407.8±8.1*	501.0±3.8*†	597.3±3.7*†	-
	<b>LZR</b>	1.0±0.1†	1.2±0.1†	1.3±0.1†	1.1±0.1†	1.5±0.1†

<b>Insulin (ng/ml)</b>	<b>OZR</b>	3.5±0.1*	5.0±0.1*	7.6±0.2*	7.8±0.1*	10.8±0.6*
	<b>OZR+HYD</b>	3.9±0.1*†	5.5±0.3*	8.1±0.3*†	9.5±0.3*†	-
	<b>OZR+CAP</b>	3.5±0.2*	3.7±0.3*†	5.4±0.3*†	6.7±0.2*†	-
	<b>OZR+GEM</b>	4.4±0.2*†	5.7±0.3*†	7.3±0.3*	8.6±0.3*†	-
	<b>OZR+ATOR</b>	3.7±0.2*	4.4±0.1*†	5.7±0.3*†	6.3±0.2*†	-
	<b>OZR+MET</b>	3.4±0.2*	-	4.3±0.1*†	5.3±0.1*†	-
	<b>OZR+ROSI</b>	3.5±0.1*	-	4.0±0.1*†	5.1±0.1*†	-
	<b>OZR+TEM</b>	3.4±0.3*	5.2±0.3*	8.1±0.5*	9.9±0.3*†	-
	<b>OZR+LNM</b>	3.9±0.2*	5.8±0.3*	9.9±0.2*†	11.3±0.4*†	-
<b>Glucose (mg/dL)</b>	<b>LZR</b>	93.7±1.1†	98.4±1.1†	100.9±1.1†	100.2±1.4†	104.7±2.0†
	<b>OZR</b>	99.7±1.4*	118.6±3.4*	138.6±2.7*	179.1±1.2*	182.6±2.7*
	<b>OZR+HYD</b>	101.0±1.8*	104.5±2.5*†	134.2±3.8*	170.5±3.3*	-
	<b>OZR+CAP</b>	99.0±3.5*	100.0±2.5†	123.5±2.5*†	137.5±5.3*†	-
	<b>OZR+GEM</b>	100.9±2.6*	105.2±2.3*†	126.0±3.5*†	170.2±3.1*	-
	<b>OZR+ATOR</b>	96.2±1.1*	109.8±2.2*†	128.7±2.2*†	159.1±3.5*†	-
	<b>OZR+MET</b>	123.7±2.1*†	-	121.8±1.5*†	132.5±2.3*†	-
	<b>OZR+ROSI</b>	121.5±0.9*†	-	118.0±1.8*†	126.8±3.3*†	-
	<b>OZR+TEM</b>	97.5±4.1*	110.8±10.9*	134.3±5.5*	170.5±4.5*	-
	<b>OZR+LNM</b>	95.5±1.7*	123.3±6.4*	149.5±3.9*	174.8±4.0*	-

**Table 3-4: Skeletal muscle vascular component data**

Skeletal muscle vascular component data, presented as mean $\pm$ SE<sup>246</sup>., for the animal groups of the present study across all age. \*  $p < 0.05$  vs. LZR at that age; †  $p < 0.05$  vs. OZR at that age.

Component	Group	7 wk	10 wk	13 wk	17 wk	20 wk
<b>Acetylcholine Dilation (<math>\mu\text{m}</math>)</b>	LZR	119.2 $\pm$ 1.1	125.0 $\pm$ 1.1 $\dagger$	129.3 $\pm$ 1.2 $\dagger$	136.5 $\pm$ 2.0 $\dagger$	139.9 $\pm$ 1.6 $\dagger$
	OZR	115.3 $\pm$ 1.9	118.4 $\pm$ 3.2*	120.5 $\pm$ 2.8*	122.6 $\pm$ 2.9*	119.3 $\pm$ 3.3*
	OZR+HYD	117.6 $\pm$ 2.6	127.3 $\pm$ 2.2 $\dagger$	131.7 $\pm$ 2.3 $\dagger$	129.6 $\pm$ 3.4*	-
	OZR+CAP	118.3 $\pm$ 2.7	117.0 $\pm$ 2.1*	124.8 $\pm$ 3.9	124.3 $\pm$ 1.9*	-
	OZR+GEM	125.5 $\pm$ 3.1 $\dagger$	126.0 $\pm$ 1.8 $\dagger$	122.1 $\pm$ 2.9*	121.6 $\pm$ 2.9*	-
	OZR+ATOR	124.0 $\pm$ 3.4* $\dagger$	129.1 $\pm$ 2.7 $\dagger$	129.3 $\pm$ 2.9 $\dagger$	134.6 $\pm$ 2.7 $\dagger$	-
	OZR+TEM	113.8 $\pm$ 4.8*	120.5 $\pm$ 2.2	119.5 $\pm$ 5.6*	118.8 $\pm$ 5.4*	-
	OZR+LNM	99.3 $\pm$ 4.3* $\dagger$	99.25 $\pm$ 4.2* $\dagger$	109.5 $\pm$ 6.3* $\dagger$	108.5 $\pm$ 1.7* $\dagger$	-
<b>Microvessel Density (#/mm<sup>2</sup>)</b>	LZR	809.9 $\pm$ 13.9	810.4 $\pm$ 13.1	811.8 $\pm$ 11.9 $\dagger$	863.1 $\pm$ 4.6 $\dagger$	823.0 $\pm$ 9.1 $\dagger$
	OZR	805.4 $\pm$ 25.2	782.4 $\pm$ 26.1	706.9 $\pm$ 16.9*	656.3 $\pm$ 20.5*	635.9 $\pm$ 11.6*
	OZR+HYD	881.4 $\pm$ 10.8* $\dagger$	874.6 $\pm$ 14.6* $\dagger$	832.3 $\pm$ 21.5 $\dagger$	869.4 $\pm$ 17.3 $\dagger$	-
	OZR+CAP	833.3 $\pm$ 12.3	813.3 $\pm$ 5.5	764.0 $\pm$ 8.0* $\dagger$	730.5 $\pm$ 16.6* $\dagger$	-
	OZR+GEM	830.2 $\pm$ 16.5	770.2 $\pm$ 12.8*	688.0 $\pm$ 11.6*	660.2 $\pm$ 10.9*	-
	OZR+ATOR	806.4 $\pm$ 8.4	803.4 $\pm$ 4.3	785.2 $\pm$ 5.0* $\dagger$	769.1 $\pm$ 7.1* $\dagger$	-
	OZR+TEM	839.0 $\pm$ 6.2*	841.4 $\pm$ 7.3* $\dagger$	850.2 $\pm$ 9.6* $\dagger$	814.1 $\pm$ 6.3* $\dagger$	-
	OZR+LNM	833.3 $\pm$ 7.8	798.5 $\pm$ 21.3	722.3 $\pm$ 12.0*	638.5 $\pm$ 8.3* $\dagger$	-
<b>Stress vs Strain <math>\beta</math></b>	LZR	2.6 $\pm$ 0.1	2.6 $\pm$ 0.1 $\dagger$	2.8 $\pm$ 0.1 $\dagger$	3.1 $\pm$ 0.1 $\dagger$	3.2 $\pm$ 0.1 $\dagger$
	OZR	2.4 $\pm$ 0.3	3.4 $\pm$ 0.5*	4.1 $\pm$ 0.6*	6.2 $\pm$ 0.4*	5.7 $\pm$ 0.7*

	OZR+HYD	3.7±0.3*	3.5±0.3*	3.8±0.4*	4.0±0.3*†	-
	OZR+CAP	3.2±0.2*	3.5±0.3*	4.2±0.2*	4.8±0.3*†	-
	OZR+GEM	3.0±0.1*	4.0±0.2*	5.7±0.3*†	6.4±0.1*	-
	OZR+ATOR	3.1±0.1*†	3.8±0.3*	5.1±0.2*	5.0±0.3*†	-
	OZR+TEM	3.4±0.6*†	3.8±0.2*	4.4±0.2*	6.3±0.1*	-
	OZR+LNM	3.4±0.2*†	4.4±0.2*†	5.5±0.3*†	7.0±0.2*†	-

**Table 3-5: Cerebral vascular component data**

Cerebral vascular component data, presented as mean±SE, for the animal groups of the present study across all age. \* p<0.05 vs. LZR at that age; † p<0.05 vs. OZR at that age.

Component	Group	7 wk	10 wk	13 wk	17 wk	20 wk
<b>Acetylcholine Dilation (µm)</b>	LZR	135.2±1.3†	144.1±0.9†	151.8±0.8†	155.0±1.4†	163.0±1.1†
	OZR	122.4±1.3*	128.4±1.0*	125.1±0.8*	122.9±1.7*	119.8±2.5*
	OZR+HYD	117.6±2.6	-	131.7±2.3†	129.6±3.4*	-
	OZR+CAP	137.5±0.7	-	139.0±0.7*	132.5±2.4*	-
	OZR+MET	133.2±0.9†	-	134.2±0.9*†	132.3±1.6*†	-
	OZR+ROSI	134.6±0.5†	-	135.7±1.7*†	127.5±1.2*†	-
	OZR+TEM	135.3±0.3†	-	133.7±1.6*†	134.2±1.6*†	-
	OZR+LNM	126.2±0.9*	-	117.3±2.5*†	112.8±1.2*†	-
<b>Microvessel Density (#/mm<sup>2</sup>)</b>	LZR	290.0±1.9†	293.0±2.1†	303.8±1.2†	313.6±1.4†	319.6±1.0†
	OZR	274.0±3.2*	270.1±2.6*	255.8±2.6*	249.1±2.1*	242.0±1.9*



	OZR+HYD	341.0±3.0*†	-	308.3±2.0†	279.7±2.1*†	-
	OZR+CAP	337.3±2.7*†	-	332.0±1.7*†	310.3±2.2†	-
	OZR+MET	329.0±2.4*†	-	334.7±3.2*†	322.3±2.3†	-
	OZR+ROSI	333.3±2.5*†	-	309.7±3.4†	322.0±2.6†	-
	OZR+TEM	341.7±1.2*†	-	341.0±1.2*†	333.3±2.8†	-
	OZR+LNM	331.2±1.6	-	305.0±1.8†	257.3±1.1*	-
<b>Stress vs Strain</b> <b>β</b>	LZR	1.6±0.1	1.7±0.1†	1.8±0.1†	2.0±0.1†	2.2±0.1†
	OZR	1.8±0.1	2.1±0.1*	2.8±0.2*	4.0±0.2*	5.4±0.1*
	OZR+HYD	3.7±0.3*	-	3.8±0.4*	4.0±0.3*†	-
	OZR+CAP	2.5±0.1*†	-	3.3±0.1*†	4.7±0.1*†	-
	OZR+MET	2.5±0.1*†	-	3.5±0.1*†	6.0±0.1*†	-
	OZR+ROSI	2.6±0.1*†	-	3.5±0.1*†	6.1±0.1*†	-
	OZR+TEM	2.5±0.1*†	-	3.4±0.1*†	5.6±0.1*†	-
	OZR+LNM	2.6±0.1	-	4.5±0.1*†	7.1±0.2*†	-

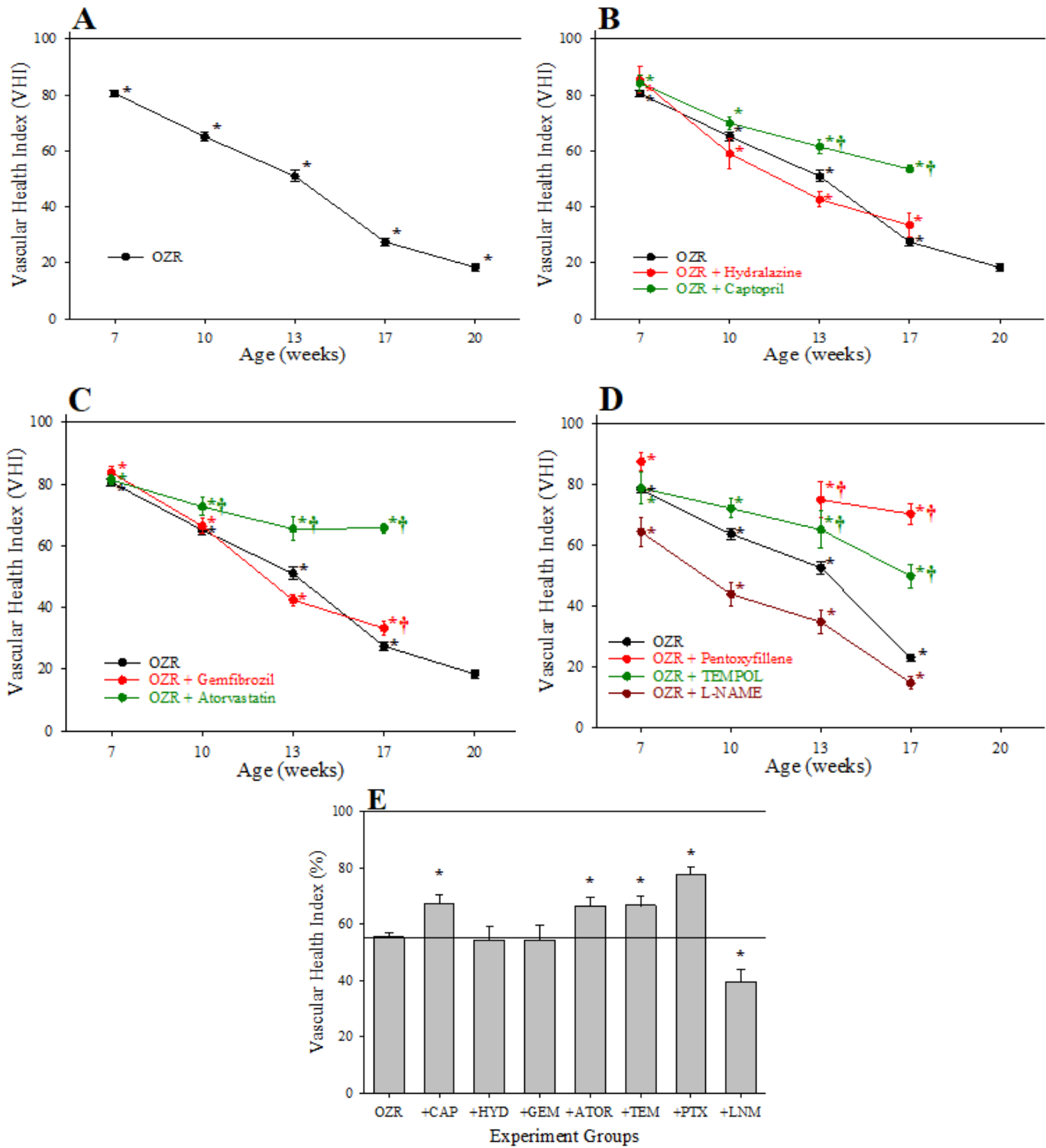
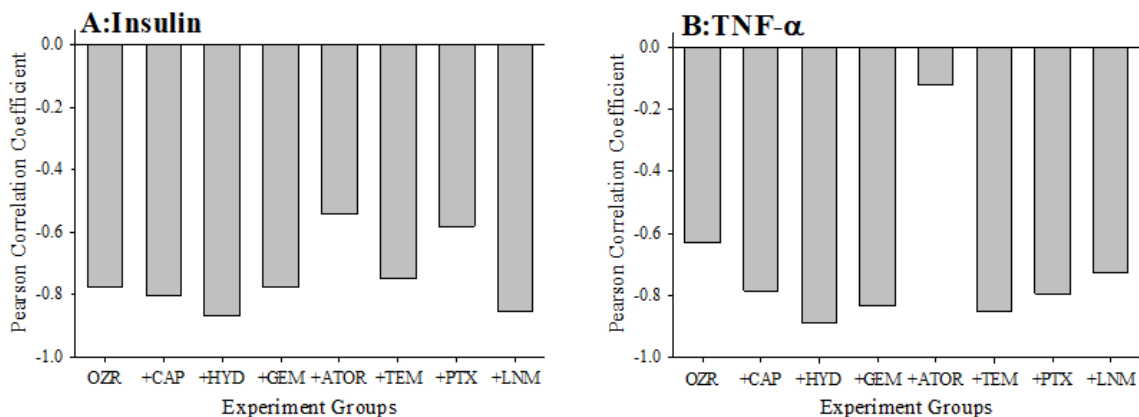


Figure 3-2: 3 parameter VHI data in skeletal muscle microcirculation

*Data describing the three-parameter determination of Vascular Health Index (VHI) within the skeletal muscle microcirculation. Data (mean±SE) are presented for OZR over the age ranges of the present study (Panel A) or the impact of chronic anti-hypertensive (Panel B), anti-dyslipidemia (Panel C), or antioxidant/anti-inflammatory/nitric oxide bioavailability (Panel D) therapies. Panel E presents the aggregate VHI from the different animal groups where all ages have been compiled into one data point. By definition, VHI from LZR is set to 100%. \*  $p < 0.05$  vs. LZR at that age; †  $p < 0.05$  vs. OZR at that age. Please see text for details.*

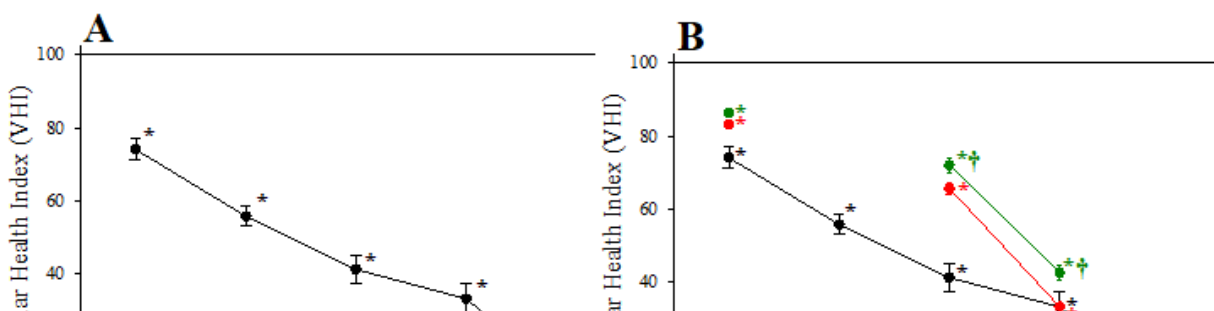
Figure 2 summarizes the data across the conditions of the present study for the calculation of the VHI in the skeletal muscle vasculature. Panel A present the data from untreated OZR in relation to the healthy control, the untreated, age-matched LZR, where VHI fell steadily with increasing severity and duration of the metabolic disease. Treatment with the anti-hypertensive agents hydralazine or captopril (Panel B) resulted in differential effects in terms of skeletal muscle VHI, where captopril resulted in a consistent blunting of the reduction to VHI, while hydralazine was without consistent impact. Panel C presents the results on skeletal muscle VHI for OZR treated with the anti-dyslipidemia agents gemfibrozil and atorvas. Panel D presents the impact of agents targeting chronic pro-oxidant (TEMPOL) and pro-inflammatory (pentoxifylline) environments in OZR. Both agents were highly effective at reducing the decline in skeletal muscle VHI across the age range of the present study. In addition, treatment of OZR with L-NAME (to remove nitric oxide bioavailability and accelerate the impact of chronic metabolic disease) increased the rate of decline in VHI across all ages of OZR. Panel E presents the time-averaged changes in VHI in OZR under the different interventions in the present study as compared to that for control LZR, and clearly demonstrates that treatment with captopril, atorvastatin, TEMPOL and pentoxifylline were most effective at improving vascular outcomes.



**Figure 3-3: TNF- and plasma insulin correlations with peripheral VHI**

*Data describing the criterion validity between plasma insulin (Panel A) or TNF- $\alpha$  (Panel B) and the skeletal muscle Vascular Health Index (VHI) across the different treatment groups in the present study. Criterion validity is demonstrated by a strong, negative Pearson Correlation coefficient between insulin or TNF- $\alpha$  and VHI in OZR. Please see text for details.*

Figure 3 presents the criterion validity for the calculations of the peripheral VHI in the present study through determination of the Pearson Correlation Coefficients with plasma insulin and TNF- $\alpha$  levels; both well-established markers of metabolic disease severity. Both plasma insulin (Panel A) and TNF- $\alpha$  (Panel B) concentrations were strongly and negatively correlated with the VHI. This correlation reflects the strong tendency for OZR with healthier vasculature and higher VHI will have the lowest insulin resistance and chronic inflammation. The exception to this pattern is with the correlation between TNF- $\alpha$  and VHI under following treatment with atorvastatin, which was much weaker, indicating a much improved overall vascular health through the measured parameters.



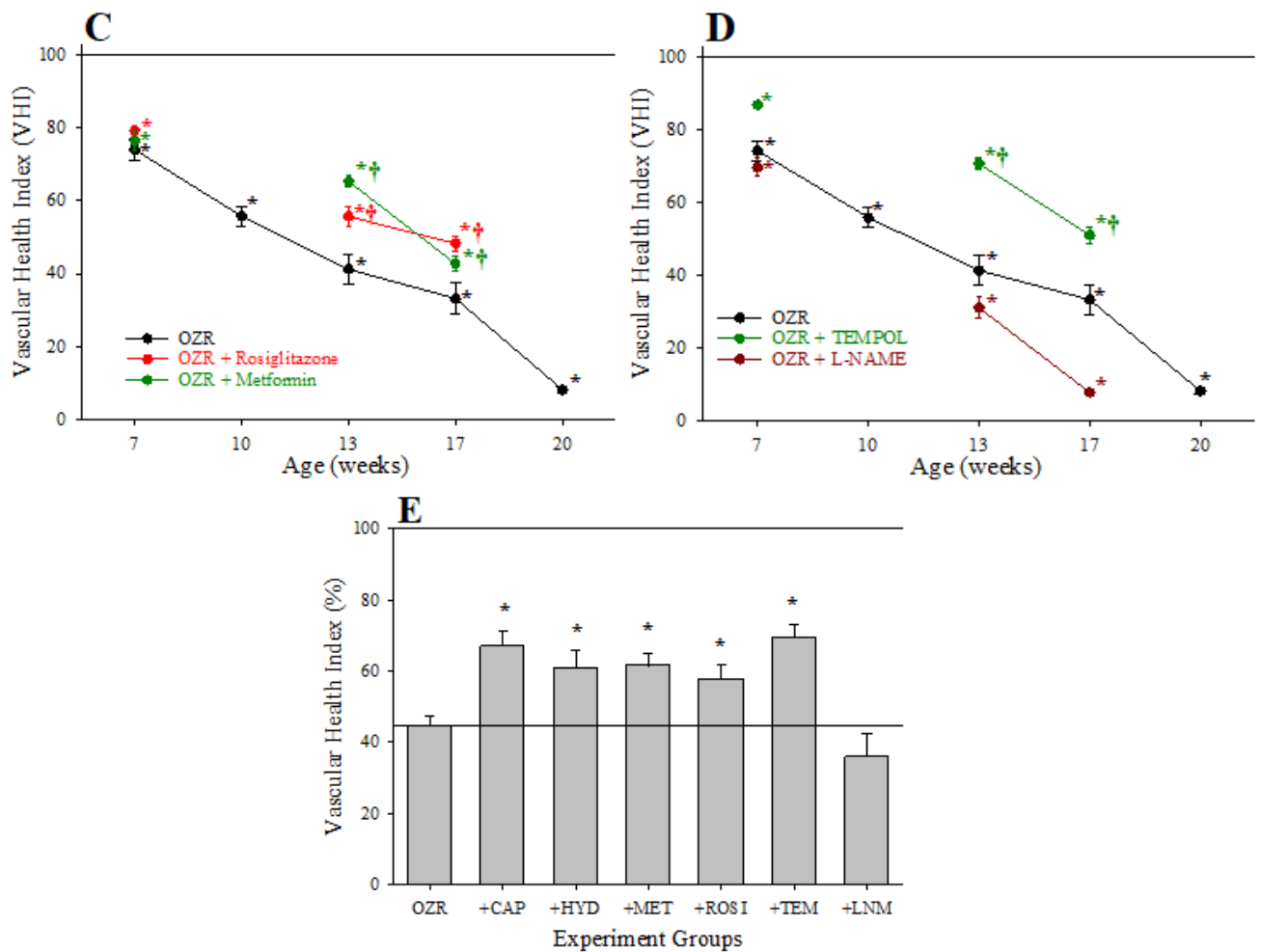


**Figure 3-4: Cerebral microcirculation VHI data**

*Data describing the three-parameter determination of Vascular Health Index (VHI) within the cerebral microcirculation. Data (mean±SE) are presented for OZR over the age ranges of the present study (Panel A) or the impact of chronic anti-hypertensive (Panel B), anti-diabetic (Panel C), or antioxidant/anti-inflammatory/nitric oxide bioavailability (Panel D)*

*therapies. Panel E presents the aggregate VHI from the different animal groups where all ages have been compiled into one data point. By definition, VHI from LZR is set to 100%. \*  $p < 0.05$  vs. LZR at that age; †  $p < 0.05$  vs. OZR at that age. Please see text for details.*

Figure 4 presents the calculations of cerebral VHI in OZR under the conditions of the present study. Panel A presents the progressive deterioration in cerebral VHI in OZR versus LZR out to 20 weeks of age. Chronic treatment with the antihypertensive agents (Panel B) or with the anti-diabetic agents (to improve glycemic control, Panel C) resulted in temporary improvements to cerebral VHI, although the results suggest that this effect may be insufficient to maintain VHI over time. A similar general pattern was determined for cerebral VHI in OZR following treatment with the antioxidant TEMPOL (Panel D), where beneficial effects on vascular health appeared to decay with increasing severity and duration of metabolic disease. Reducing nitric oxide bioavailability with L-NAME resulted in significant reductions to VHI in comparison to untreated OZR, accelerating the progression of cerebrovasculopathy. The time-averaged VHI for the cerebral circulation of OZR under the conditions of the present study are summarized in Panel E, where the employed interventions improved the aggregate VHI as compared to that in OZR.

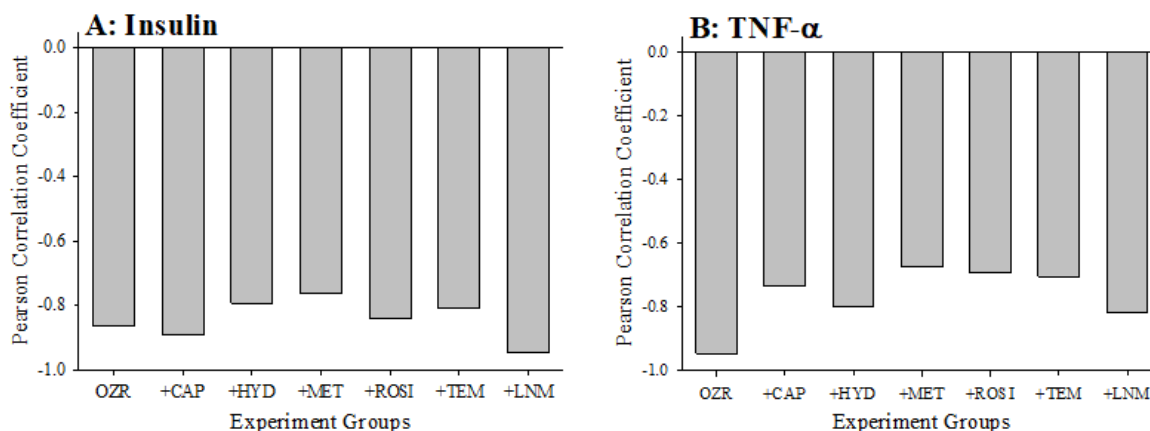


**Figure 3-5: TNF- and plasma insulin correlations with cerebral VHI**

*Data (describing the criterion validity between plasma insulin (Panel A) or TNF- $\alpha$  (Panel B) and the cerebral Vascular Health Index (VHI) across the different treatment groups in the present study. Criterion validity is demonstrated by a strong, negative Pearson Correlation coefficient between insulin or TNF- $\alpha$  and VHI in OZR.*

The criterion validity for the calculations of cerebral VHI in the present study with plasma insulin and TNF- $\alpha$  levels are presented in Figure 5. Both plasma insulin (Panel A) and TNF- $\alpha$  (Panel B) concentrations were strongly and negatively correlated with the VHI and this was demonstrated across all interventions. Comparable to the interpretation for skeletal muscle VHI, these results indicate the strong correlation between healthier vasculature and higher VHI with low levels of insulin resistance and chronic inflammation in the OZR cerebrovascular.

### 3.4 Discussion

This study describes the approach for developing and using a vascular health index (VHI) representing integrated vascular function while allowing for the pooling

of data across many different studies to maximize inferential power and available analytic approaches. We did this by using our raw data from multiple studies to calculate this new metric over the temporal development of metabolic disease in OZR and quantify the associated progressive dysfunction within the microcirculation. Additionally, we used our metric to outline the impact of three major classes of clinically relevant pharmacological interventions (anti-hypertension, anti-dyslipidemia, anti-diabetes) along with antioxidant treatment and present the relative effectiveness of each intervention in improving integrated microvascular health within the OZR manifesting metabolic disease. Throughout this process, we demonstrated the face, content, criterion and discriminant validity of the VHI; suggesting that this metric of integrated vascular function can be used for more complex analyses moving forward.

The development of the VHI has several characteristics that deserve some comment. Foremost, it is not intended to be a predictive score (such as things like the Framingham Risk Score; [27; 28]), and as such we have included no parameter weighting in its calculation. This is important to note as there is no clear *a priori* rationale justifying parameter weighting at this time and there is also no consensus regarding the relative importance of vascular reactivity, wall mechanics or microvessel density in terms of contributions to health outcomes. Finally, parameter weighting, by definition, requires the use of a regression-based approach designed to predict an outcome. As this was not the purpose of VHI, this was rejected in favor of the analytical approach employed. [3]

As presented Figure 1, the calculation of either skeletal muscle or cerebral VHI was dependent on the integration of three parameters, acetylcholine-induced dilation (as a marker of overall reactivity and endothelial function), the slope of the circumferential stress



vs. strain relation of the vascular wall (as a marker of vascular wall stiffness and overall mechanics), and microvessel density (MVD; as a central determinant of the ability of the microvascular networks to effectively deliver and exchange materials to metabolic active tissues). Each of these three markers has been well documented in the existing literature to be highly predictive of a poor vascular outcomes and the impact of cardiovascular/cerebrovascular disease risk [29; 30]. While other markers of vascular structure and function could certainly be used if desired by an investigative group to assess a different outcome, we believe that these three markers are not only relatively straightforward to determine and do cover the major aspects of vascular/microvascular health [23]. Thorough discussions of the mechanistic bases of the impact of chronic metabolic disease and the pharmacological interventions employed in the present study have been presented elsewhere and will not be covered in detail in this manuscript.

In terms of demonstrating the validity of the skeletal muscle and cerebral VHI, it is important to note that two plasma biomarkers that have been well-established indicators of chronic metabolic disease severity and duration, plasma insulin [31; 32] and TNF- $\alpha$  [32; 33] concentrations, demonstrated strong negative correlations with VHI in untreated OZR. Following the imposition of multiple pharmacological interventions used in this study, there was some reduction to the correlation coefficient, suggesting the creation of a healthier vasculature, although the clear correlations still remained, as would be expected.

In terms of discriminant validity for VHI, much of this is provided by the changes in the individual parameters comprising the index (vascular reactivity, vascular wall mechanics and microvessel density) in response to the most effective pharmacological interventions (e.g., atorvastatin and rosiglitazone). However, the use of L-NAME in OZR

deserves a brief discussion. L-NAME essentially eliminates vascular nitric oxide bioavailability and treating animals with it chronically can be considered to be a proxy for mimicking that impact of chronic metabolic disease on vascular health, albeit an accelerated one [26]. The more rapid decay in VHI in OZR with chronic L-NAME treatment is a clear demonstration of the ability of VHI to effectively discriminate between experimental conditions and different states of vascular health.

One of the most interesting aspects of the results of the present study is in regard to the timing and aggressiveness of pharmacological interventions to maintain skeletal muscle and cerebral vascular health in chronic metabolic disease. The results of the present study strongly suggest that aggressive prodromic intervention with appropriate pharmacological agents for treating risk factors such as hypertension, impaired glycemic control, atherogenic dyslipidemia and the pro-oxidant and pro-inflammatory environments that are associated with them, may be most appropriate and effective in terms of maintaining vascular health over time. From the perspective of health care delivery, while it may be more effective in terms of patient outcomes to intervene earlier with aggressive pharmacological avenues to maintain vascular health, especially given challenges in patient adherence and compliance with lifestyle changes, an aggressive early intervention may also be more economically sustainable given the exorbitant costs associated with chronic disease and end-organ damage if treatment is delayed [34; 35].

Continuing with this concept, the results of the present study also suggested pharmacological agents targeted at one risk factor (e.g., metformin or rosiglitazone) may not be adequately effective in the setting of more complicated disease risk, demonstrating a progressive inability to maintain vascular health. These results suggest that multiple

treatments may be required for realizing optimal outcomes, or that the benefits derived from pharmacological agents with pleiotropic effects such as atorvastatin [4], and to some extent anti-hypertensive agents [4], may allow for a greater maintenance of vascular health beyond that which would be expected from simple risk factor reduction alone. Recent study involving machine learning approaches have suggested these outcomes may be realized in chronic metabolic disease, where chronic interventions with pharmacological agents with beneficial impacts in addition to risk factor reduction were highly effective at improving functional outcomes that may not have been associated with the intended use of the drug [36].

A key part of proposing a novel metric assessing the relative status of a physiological system is outlining meaningful applications. [3] The demonstrated development and use of VHI allow for simple and accurate interpretations of the relative vascular health profiles and significant differences in integrated vascular health outcomes between animal models under different treatment regimes. Consequently, the development and evaluation of new pharmacological interventions addressing traditional cardiovascular disease risk factors like impaired lipid control and hypertension can benefit from a metric like VHI to guide and determine intervention's associated anti-vasculopathy capabilities. Furthermore, VHI can also be used in the study of progressing preclinical symptoms and states of low CVD risk factors to elevated CVD risk factors and actual disease diagnoses to help determine optimal windows of treatment for different interventions to achieve ideal health outcomes. Finally, the described use of VHI allows us to link datasets across time, research groups and different studies to make such assessments and comparisons of interventions and their outcomes on vascular health more accessible and manageable. The effective use of tools such as VHI can assist

investigators in better understanding of the role of vascular dysfunction in disease etiology and in assessments of the effectiveness of various interventions in addressing progressive vasculopathy.

A version of this chapter has been published: Menon NJ, Halvorson BD, Alimorad GH, Frisbee JC, Lizotte DJ, Ward AD, Goldman D, Chantler PD, Frisbee SJ. Application of a novel index for understanding vascular health following pharmacological intervention in a pre-clinical model of metabolic disease. *Front Pharmacol.* 2023 Jan 25;14:1104568. doi: 10.3389/fphar.2023.1104568. PMID: 36762103; PMCID: PMC9905672.

### 3.5 Literature Cited

- [1] A.M.A. Martins, M.U.B. Paiva, D.V.N. Paiva, R.M. de Oliveira, H.L. Machado, L. Alves, C.R.C. Picossi, A.T. Faccio, M.F.M. Tavares, C. Barbas, V.Z.R. Giraldez, R.D. Santos, G.U. Monte, and F.A. Atik, Innovative Approaches to Assess Intermediate Cardiovascular Risk Subjects: A Review From Clinical to Metabolomics Strategies. *Front Cardiovasc Med* 8 (2021) 788062.
- [2] S. Amal, L. Safarnejad, J.A. Omiye, I. Ghanzouri, J.H. Cabot, and E.G. Ross, Use of Multi-Modal Data and Machine Learning to Improve Cardiovascular Disease Care. *Front Cardiovasc Med* 9 (2022) 840262.
- [3] N.J. Menon, B.D. Halvorson, G.H. Alimorad, J.C. Frisbee, D.J. Lizotte, A.D. Ward, D. Goldman, P.D. Chantler, and S.J. Frisbee, A novel vascular health index: Using data analytics and population health to facilitate mechanistic modeling of microvascular status. *Front Physiol* 13 (2022) 1071813.
- [4] S.J. Frisbee, S.S. Singh, D.N. Jackson, K.A. Lemaster, S.A. Milde, J.K. Shoemaker, and J.C. Frisbee, Beneficial Pleiotropic Antidepressive Effects of Cardiovascular Disease Risk Factor Interventions in the Metabolic Syndrome. *J Am Heart Assoc* 7 (2018).
- [5] J.C. Frisbee, Hypertension-independent microvascular rarefaction in the obese Zucker rat model of the metabolic syndrome. *Microcirculation* 12 (2005) 383-92.
- [6] A.G. Goodwill, S.J. Frisbee, P.A. Stapleton, M.E. James, and J.C. Frisbee, Impact of chronic anticholesterol therapy on development of microvascular rarefaction in the metabolic syndrome. *Microcirculation* 16 (2009) 667-84.
- [7] P.D. Chantler, C.D. Shrader, L.E. Tabone, A.C. d'Audiffret, K. Huseynova, S.D. Brooks, K.W. Branyan, K.A. Grogg, and J.C. Frisbee, Cerebral Cortical Microvascular Rarefaction in Metabolic Syndrome is Dependent on Insulin Resistance and Loss of Nitric Oxide Bioavailability. *Microcirculation* 22 (2015) 435-45.
- [8] J.C. Frisbee, A.G. Goodwill, S.J. Frisbee, J.T. Butcher, R.W. Brock, I.M. Olfert, E.R. DeVallance, and P.D. Chantler, Distinct temporal phases of microvascular

- rarefaction in skeletal muscle of obese Zucker rats. *Am J Physiol Heart Circ Physiol* 307 (2014) H1714-28.
- [9] J.C. Frisbee, J.B. Samora, and D.P. Basile, Angiostatin does not contribute to skeletal muscle microvascular rarefaction with low nitric oxide bioavailability. *Microcirculation* 14 (2007) 145-53.
- [10] J.C. Frisbee, Impaired hemorrhage tolerance in the obese Zucker rat model of metabolic syndrome. *J Appl Physiol* (1985) 100 (2006) 465-73.
- [11] Y. Liu, K.T. Fredricks, R.J. Roman, and J.H. Lombard, Response of resistance arteries to reduced PO<sub>2</sub> and vasodilators during hypertension and elevated salt intake. *Am J Physiol* 273 (1997) H869-77.
- [12] K.T. Fredricks, Y. Liu, N.J. Rusch, and J.H. Lombard, Role of endothelium and arterial K<sup>+</sup> channels in mediating hypoxic dilation of middle cerebral arteries. *Am J Physiol* 267 (1994) H580-6.
- [13] K.T. Fredricks, Y. Liu, and J.H. Lombard, Response of extraparenchymal resistance arteries of rat skeletal muscle to reduced PO<sub>2</sub>. *Am J Physiol* 267 (1994) H706-15.
- [14] B.D. Halvorson, J.J. McGuire, K.K. Singh, J.T. Butcher, J.H. Lombard, P.D. Chantler, and J.C. Frisbee, Can Myogenic Tone Protect Endothelial Function? Integrating Myogenic Activation and Dilator Reactivity for Cerebral Resistance Arteries in Metabolic Disease. *J Vasc Res* 58 (2021) 286-300.
- [15] G.L. Baumbach, and M.A. Hajdu, Mechanics and composition of cerebral arterioles in renal and spontaneously hypertensive rats. *Hypertension* 21 (1993) 816-26.
- [16] S.D. Brooks, E. DeVallance, A.C. d'Audiffret, S.J. Frisbee, L.E. Tabone, C.D. Shrader, J.C. Frisbee, and P.D. Chantler, Metabolic syndrome impairs reactivity and wall mechanics of cerebral resistance arteries in obese Zucker rats. *Am J Physiol Heart Circ Physiol* 309 (2015) H1846-59.
- [17] W.R. Milnor, *Hemodynamics*, Williams & Wilkins, Baltimore, 1982.
- [18] A.S. Greene, J.H. Lombard, A.W. Cowley, Jr., and F.M. Hansen-Smith, Microvessel changes in hypertension measured by Griffonia simplicifolia I lectin. *Hypertension* 15 (1990) 779-83.

- [19] F. Hansen-Smith, A.S. Greene, A.W. Cowley, Jr., and J.H. Lombard, Structural changes during microvascular rarefaction in chronic hypertension. *Hypertension* 15 (1990) 922-8.
- [20] J.C. Frisbee, Remodeling of the skeletal muscle microcirculation increases resistance to perfusion in obese Zucker rats. *Am J Physiol Heart Circ Physiol* 285 (2003) H104-11.
- [21] D.H. Munzenmaier, and A.S. Greene, Chronic angiotensin II AT1 receptor blockade increases cerebral cortical microvessel density. *Am J Physiol Heart Circ Physiol* 290 (2006) H512-6.
- [22] P. Price, Jhangiani, R., & Chiang, I., *Research Methods of Psychology*, BCcampus, Victoria, BC, 2015.
- [23] R.M. Effros, H. Schmid-Schönbein, and J. Ditzel, *Microcirculation, current physiologic, medical, and surgical concepts*, Academic Press, New York, 1981.
- [24] M. Burgmaier, S. Sen, F. Philip, C.R. Wilson, C.C. Miller, 3rd, M.E. Young, and H. Taegtmeyer, Metabolic adaptation follows contractile dysfunction in the heart of obese Zucker rats fed a high-fat "Western" diet. *Obesity* 18 (2010) 1895-901.
- [25] P.J. Ebenezer, N. Mariappan, C.M. Elks, M. Haque, and J. Francis, Diet-induced renal changes in Zucker rats are ameliorated by the superoxide dismutase mimetic TEMPOL. *Obesity* 17 (2009) 1994-2002.
- [26] J.C. Frisbee, Reduced nitric oxide bioavailability contributes to skeletal muscle microvessel rarefaction in the metabolic syndrome. *Am J Physiol Regul Integr Comp Physiol* 289 (2005) R307-R316.
- [27] L.L. Cooper, S.K. Musani, J.A. Moore, V.A. Clarke, Y. Yano, K. Cobbs, C.W. Tsao, J. Butler, M.E. Hall, N.M. Hamburg, E.J. Benjamin, R.S. Vasan, G.F. Mitchell, and E.R. Fox, Clinical Associations of Vascular Stiffness, Microvascular Dysfunction, and Prevalent Cardiovascular Disease in a Black Cohort: The Jackson Heart Study. *J Am Heart Assoc* 9 (2020) e017018.
- [28] K. Sumayin Ngamdu, O.O. Adewale, I. Mallawaarachchi, O.K. Alozie, A.K. Dwivedi, and D.L. Bhatt, Association Between the Framingham Risk Score and Carotid Artery Intima-Media Thickness in Patients With Human Immunodeficiency Virus. *Am J Cardiol* 127 (2020) 156-162.

- [29] N.F. Chu, D. Spiegelman, G.S. Hotamisligil, N. Rifai, M. Stampfer, and E.B. Rimm, Plasma insulin, leptin, and soluble TNF receptors levels in relation to obesity-related atherogenic and thrombogenic cardiovascular disease risk factors among men. *Atherosclerosis* 157 (2001) 495-503.
- [30] J.L. Silveira Rossi, S.M. Barbalho, R. Reverete de Araujo, M.D. Bechara, K.P. Sloan, and L.A. Sloan, Metabolic syndrome and cardiovascular diseases: Going beyond traditional risk factors. *Diabetes Metab Res Rev* 38 (2022) e3502.
- [31] N. Vogelzangs, C.J.H. van der Kallen, M.M.J. van Greevenbroek, B.W. van der Kolk, J.W.E. Jocken, G.H. Goossens, N.C. Schaper, R.M.A. Henry, S. Eussen, A. Valsesia, T. Hankemeier, A. Astrup, W.H.M. Saris, C.D.A. Stehouwer, E.E. Blaak, I.C.W. Arts, and c. Diogenes, Metabolic profiling of tissue-specific insulin resistance in human obesity: results from the Diogenes study and the Maastricht Study. *Int J Obes (Lond)* 44 (2020) 1376-1386.
- [32] M. Koenen, M.A. Hill, P. Cohen, and J.R. Sowers, Obesity, Adipose Tissue and Vascular Dysfunction. *Circ Res* 128 (2021) 951-968.
- [33] E.J. Barrett, Z. Liu, M. Khamaisi, G.L. King, R. Klein, B.E.K. Klein, T.M. Hughes, S. Craft, B.I. Freedman, D.W. Bowden, A.I. Vinik, and C.M. Casellini, Diabetic Microvascular Disease: An Endocrine Society Scientific Statement. *J Clin Endocrinol Metab* 102 (2017) 4343-4410.
- [34] L.M.M. Janssen, M. Hiligsmann, A.M.J. Elissen, M.A. Joore, N.C. Schaper, J.H.A. Bosma, C.D.A. Stehouwer, S.J.S. Sep, A. Koster, M.T. Schram, and S. Evers, Burden of disease of type 2 diabetes mellitus: cost of illness and quality of life estimated using the Maastricht Study. *Diabet Med* 37 (2020) 1759-1765.
- [35] J. Rangaswami, K. Tuttle, and M. Vaduganathan, Cardio-Renal-Metabolic Care Models: Toward Achieving Effective Interdisciplinary Care. *Circ Cardiovasc Qual Outcomes* 13 (2020) e007264.
- [36] M.M. Nowak, M. Niemczyk, M. Florczyk, M. Kurzyna, and L. Paczek, Effect of Statins on All-Cause Mortality in Adults: A Systematic Review and Meta-Analysis of Propensity Score-Matched Studies. *J Clin Med* 11 (2022).



## 4 Conclusion

In this thesis, we have outlined an approach to establish and validate a composite metric of vascular function to ultimately facilitate the study of vascular dysfunction. The utility of an integrated measure of vascular health will be most evident in studies looking to investigate vascular dysfunction and its role in disease etiology, its response to treatments and so on. Our research has been conducted using a novel vascular health index which we have developed to provide an integrated and wholistic picture of vascular function. The purpose of this conclusion is to integrate the discussions of our two papers and highlight the key findings and contributions of our research.

In the second chapter, we developed a novel vascular health index to facilitate mechanistic modeling of microvascular status. To begin with, it was important to determine and explain the utility of VHI in comprehending vasculopathy. When evaluating a new metric for assessing an integrated biological system, it is crucial to comprehend how the metric adds value beyond the individual components that make up the metric. VHI allows for an accurate and more holistic determination of vascular health in animal models and identification of significant differences between cohorts. It also facilitates comparison of outcomes across time, experiments, and research groups. Used alongside established disease risk scores and relevant biomarkers, VHI can analyze relationships between vascular health and chronic conditions, sexual dimorphism, and chronic interventions, and identify potential subgroups within datasets to improve understanding of disease development through the lens of vascular dysfunction.

Some of the possible implications of our research for the field of vascular health may be discerned by conducting broader correlations tests – like we did to show criterion validity – to see if our VHI has significant and predicable relationships with various biomarkers of vascular dysfunctions and/or behavioral outcomes in chronic conditions like depression. Such work could facilitate useful predictive modelling using VHI.

There are also some limitations to the work presented in this thesis that should be highlighted. Firstly, it should be mentioned that while the method and setup for our index is applicable to other models of vasculopathy – given that it is based on relative deviations from healthy control subjects – the specific validity of any adapted version of VHI applied to other models of vasculopathy (outside of OZR) will have to similarly be demonstrated before use. Another limitation and factor to consider when using VHI is has to do with the percentile-based component scores described in chapter 3 which was implemented to circumvent differing ranges of component scores which may artificially place importance on some of the VHI components. This limitation being that the use of VHI must preceded by the verification of similar variances across all component scores of VHI and the presence of large and representatively distributed dataset of subjects. Another possible limitation to consider maybe the use of two different staining targets used to measure micro vessel density in the brain and peripheral tissue which makes comparisons between cerebral and peripheral VHI profiles less tenable. Another possible limitation to consider is that the effect that aging has on healthy control lean Zucker rats is somewhat hidden in our method of VHI calculation.

We have demonstrated the utility of our novel vascular health index in evaluating disease etiology and the role of vascular dysfunction in various pathologies. However, we also

acknowledge that the index should not be considered in isolation but in conjunction with the individual components that make up the index as well as any other relevant measures of vascular function as it is important to discern the specific degrees of impact that deficits to vascular reactivity, vascular wall mechanics and network health have on vascular health. In the same breath, VHI itself is best used as a complimentary tool because it provides a broader context that none of its individual components can provide in isolation. Additionally, in our third chapter we have shown how our index can be used in developing pharmacological treatments and assessing the effectiveness of various treatments. The study results showed the relative effectiveness of interventions with diverse mechanisms in preserving the vascular health index of cerebral or skeletal muscle in aging obese Zucker rats. The findings also reveal the relative advantage of certain pharmacological agents in terms of vascular health outcomes, despite their similar effectiveness in targeting the intended outcomes/associated symptoms of metabolic disease. The study also drives home the utility of a more comprehensive approach to examining microvasculopathy in settings of elevated disease risk and following pharmacological interventions, as it makes the study of intervention timing, efficacy, and development of more accessible and manageable.

VHI is a tool to be used in the study cerebrovascular diseases and chronic conditions such as depression that are underpinned by vascular dysfunction. In the context of depression, VHI may provide a useful tool for basic scientists exploring the role of vascular dysfunction in the development of depressive symptoms, while also facilitating the development of more effective treatment strategies that target both the psychiatric and vascular components of the disorder. Overall, the use of VHI alongside other markers of

vascular health, represents a promising approach for studying cerebrovascular diseases and chronic conditions that are associated with vascular dysfunction, potentially improving our ability to diagnose and treat these conditions.

## Curriculum Vitae

**Name:** Nithin Jayadevan Menon, BSc

**Title:** M.Sc. Graduate Student, Department of Medical Biophysics University of Western Ontario; Schulich School of Medicine and Dentistry

**Education:**

2017-2021 University of Western Ontario BMSc. (Medical Biophysics)

2021-present University of Western Ontario M.Sc. (Medical Biophysics) *Supervisor:* Jefferson Frisbee

**Academic Honors and Professional Recognition:**

Ontario Graduate Scholarship - Masters (\$15 000) 2022-2023

Dean's Honor List 2018-2022

Western Entrance Scholarship (\$10 000) 2017-2021

### PUBLICATION HISTORY

**Peer-Reviewed Manuscripts:**

**Menon NJ**, Halvorson BD, Alimorad GH, Frisbee JC, Lizotte DJ, Ward AD, Goldman D, Chantler PD, Frisbee SJ. A novel vascular health index: Using data analytics and population health to facilitate mechanistic modeling of microvascular status. *Front Physiol.* 2022 Dec 6;13:1071813. doi: 10.3389/fphys.2022.1071813. PMID: 36561210; PMCID: PMC9763931.

**Menon NJ**, Halvorson BD, Alimorad GH, Frisbee JC, Lizotte DJ, Ward AD, Goldman D, Chantler PD, Frisbee SJ. Application of a novel index for understanding vascular health following pharmacological intervention in a pre-clinical model of metabolic disease. *Front Pharmacol.* 2023 Jan 25;14:1104568. doi: 10.3389/fphar.2023.1104568. PMID: 36762103; PMCID: PMC9905672.

Halvorson BD, **Menon NJ**, Goldman D, Frisbee SJ, Goodwill AG, Butcher JT, Stapleton PA, Brooks SD, d'Audiffret AC, Wiseman RW, Lombard JH, Brock RW, Olfert IM, Chantler PD, Frisbee JC. The development of peripheral microvasculopathy with chronic metabolic disease in obese Zucker rats: a retrograde emergence? *Am J Physiol Heart Circ Physiol.* 2022 Sep 1;323(3):H475-H489. doi: 10.1152/ajpheart.00264.2022. Epub 2022 Jul 29. PMID: 35904886; PMCID: PMC9448278.

Schonberger ZG, Huang SJY, Thakkar RN, Mamone AA, Khan DI, Chow NLY, Ahmed M, Sivaram N, Bao Y, Kesavan V, Côté J, Sun C, Chhina J, Halvorson

BD, Alimorad GH, **Menon NJ**, Goldman D, Frisbee SJ. Assessments of Perfusion, Blood Flow, and Vascular Structure in Ambulatory Subjects: Guidance for Translational Research Scientists. *J Vasc Res.* 2023 Feb 24;1-57. doi: 10.1159/000527765. Epub ahead of print. PMID: 36843014.

**Published Abstracts:**

Frisbee SJ, **Menon NJ**, Halvorson BD, Alimorad GH, Frisbee JC, Lizotte D, Ward A, Goldman D. Application of a novel index for understanding vascular health following pharmacological intervention in a pre-clinical model of metabolic disease. European Society for Microcirculation Biannual Meeting. Aarhus, Denmark, April 24-27, 2023.

**Seminars:**

“Application of a novel index for understanding vascular health following pharmacological intervention in a pre-clinical model of metabolic disease”. Department of Medical Biophysics, University of Western Ontario, London, ON, 2021